KAZAKH-BRITISH TECHNICAL UNIVERSITY
SCHOOL OF INFORMATION AND TECHNOLOGY

Automation of standard technological processes and manufacturing

**DEVELOPMENT OF AN AUTOMATED CLIMATE CONTROL SYSTEM FOR A GRAIN STORAGE FACILITY BASED ON THE SMART CITY CONCEPT**


| | |
|---|---|
| Prepared by: | Masimba C. |
| Checked by: | Samigulina Z.I. |
| PhD (docent), | |
| Prof of SITE | |


Almaty, 2025

CONTENT

## INTRODUCTION

Grain storage plays a critical role in the economies of the developed and developing countries. Therefore its essential to provide a proper monitoring of the grain storage facility to reduce the grain loss. The current grain storage facility involves a lot of human efforts in all the activities and this reduces efficiency and increases the time consumption [1]. In the proposed projects these challenges are analyzed and solved. In this project a fully automated grain storage system using PLC and SCADA is proposed. The main objective of the research is control and maintain parameters such as temperature and humidity using automated system that is based on a smart city. Implementing this prevents the formation of micro-organisms that will spoil the grains. The main parameter that is essential for proper storage of grains is temperature which is taken as the input parameter to be controlled using PLC. The Scada system acquires the required data and monitors the overall process [2].

In this project an automated system for heating, ventilation and air conditioning process for the grain storage facility is developed. In this project a heat exchanger was selected as the control object. A mathematical model of the control object was formulated and it was important for stability, controllability and observability. The PID regulator was implemented and its coefficients were developed.

The technological process will involve the provision of a remote detection of oil leakage from the main pipelines. Using the SCADA system the changes in all the pumping technological parameters in real time as described are monitored. The mathematical formulation of the problem for controlling the operating modes of the technological objects and the main storage facility was also obtained [3]. The research proposes the use of temperature sensors and provides methods of detecting humid and low temperatures in the grain storage facilities. Using PLC, the data received from the temperature and detect if there are any variations is analyzed. In case of any variations then it means that there are high humid which might affect the grains.

## 1. Technological part

Among all the technologies, the real time monitoring of grain temperature and moisture inside the silos was considered as one of the most critical factors for effective storage [8]. It played a pivotal role in early warning for food safety, preservation of grain quality and guiding aeration and energy-saving strategies and solutions. The temperature and moisture of the stored grain exhibited pronounced spatial variability. In this research work the distributed temperature monitoring is implemented. This will be done using the cable-based systems which are equipped with the thermistors, thermocouples and digital temperature sensors.

The grain dryer control system in the Silo is evolving towards multifunctioning integration and modular design. The system will be able to automatically adjust according to the drying requirements of different types of grain. This ensures that the machine can achieve multiple functions. On the other hand, the modular design makes the system upgrades and maintenance more convenient. This allows the user to replace or upgrade specific modules based on their needs. This enhances the system's flexibility and adaptability.

### 1.1 Description of the technological process for the automation climate system monitoring system in a grain storage facility

In the proposed system, the temperature and humidity are maintained at an optimum temperature and humidity based on the grain type. The main component is the heat exchanger which will be used to control the temperature and dehumidification of the grain storage facility. Air conditioners work by extracting heat from indoor air and expelling it outdoors. This process generates cool air that is then circulated throughout the space, effectively lowering the temperature. The heat exchanger is the core component responsible for this heat transfer, and its efficiency directly determines the unit's overall cooling performance.

A heat exchanger is a device that facilitates heat transfer between two fluids without allowing them to mix [9]. Its performance depends on several factors, including temperature differential, heat transfer surface area, fluid flow rates, and flow configurations. Heat exchangers are essential across diverse industries, such as petroleum refining, food processing, petrochemicals, power generation, nuclear energy, and aerospace applications. Among various types, shell-and-tube heat exchangers are the most widely used due to their ability to handle a broad range of temperatures and pressures. This is the heat exchanger that is used in the research project. Compared to double-pipe designs, they provide a higher surface-to-volume ratio and can be easily manufactured in various sizes and configurations. These exchangers are robust under high pressure, and their modular design allows straightforward disassembly for maintenance and cleaning.

A shell-and-tube heat exchanger evolves from the basic double-pipe concept. Instead of a single tube inside a larger pipe, it consists of multiple tubes bundled within a cylindrical shell. One fluid flows inside the tubes, while the other circulates around them in the space between the tubes and the shell. In grain storage facilities, HVAC systems play a critical role in maintaining food safety, quality, and operational efficiency. They precisely control temperature and humidity to create optimal conditions for storage, processing, and preservation—preventing spoilage, extending shelf life, and ensuring compliance with regulatory standards—while also promoting energy efficiency and sustainability.

The RF module acts as a transmitter to transmit data from the sensors to the controller which in this case is the Schneider PLC. The temperature sensor module is connected to the PLC end and then it acts as a receiver and a data is then fed to the PLC. In the PLC, an acceptable range of temperature data is set. The humidity sensors module is also connected to the PLC to monitor the humidity levels. The system runs on real-time. Whenever there is a change in humidity levels and temperate it means there is a high humidity and unacceptable temperature which needs to be regulated to optimum levels. The PLC will detect the difference in temperature and humidity levels across the acceptable range. This will generate an alarm in the PLC-HMI. In case the temperature and humidity levels is high then the alarm will be set as a high priority on the other hand of the leakage is low then the alarm will be set as a low priority [13].

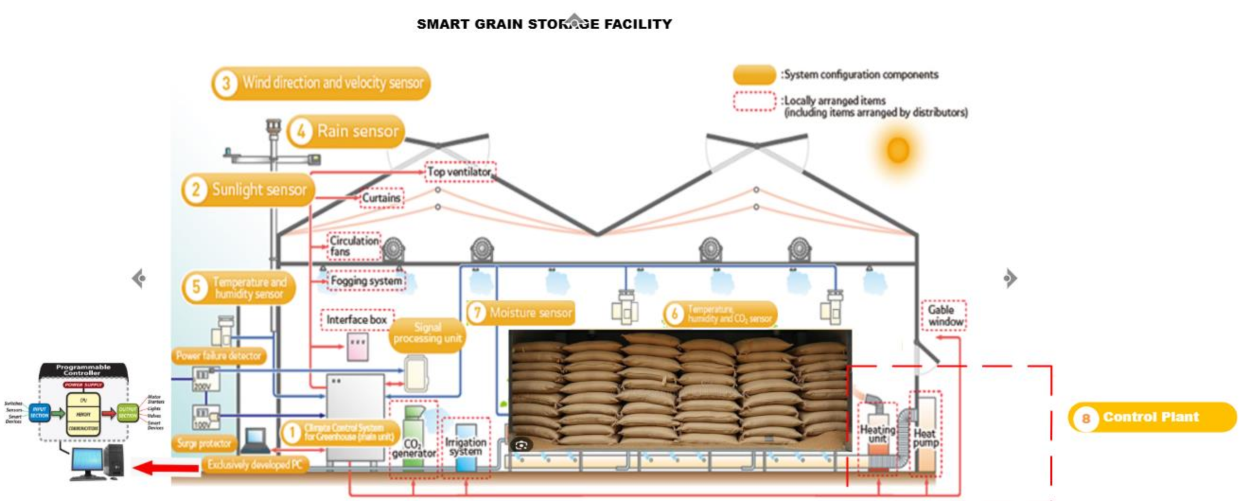

Figure 1.1 - Process flow visualization diagram

The simulation was performed on MatLab Simulink to ensure that the performance of the controller meets the requirements. The controller was done using ZN (Zieglar and Nicholas ) PID. In the research a new technique based on the autoregressive and data analysis of the humidity and temperature data to determine the leakage and decision to be made instantly to control the leakage in the pipes is developed. The numerical results demonstrated that the proposed technique was able to detect the leakage in the presence of uncertainty. The detects and the estimates leaks were very accurately. The pipeline model equations using the ARX-Laguerre technique is developed. Therefore, the proposed algorithm will be based on the ARX-Laguerre fuzzy PID Algorithm to detect and locate the leaks in the pipeline. For analysis a comparison of this method with the rest of the methods was performed [6].

The figure above shows an automated climate control system for a grain storage facility, developed under the smart city concept, establishes a robust, intelligent framework to maintain optimal environmental conditions and safeguard post-harvest grain quality in urban and peri-urban settings. At its foundation lies a smart grid power supply system that ensures uninterrupted, demand-responsive electricity by integrating with municipal energy networks. This enables dynamic load management and incorporation of renewable micro-sources to achieve near-100% operational reliability while aligning with city-wide sustainability goals.

Central to the architecture is a Programmable Logic Controller (PLC). This serves as the primary processing unit, that receives a real-time data from distributed sensors monitoring temperature, relative humidity, and grain moisture content. This data is transmitted wirelessly using Modbus Protocol cause of using Schneiderlin PLC system, which not only connects field devices to the PLC but also interfaces with the broader municipal IoT infrastructure, facilitating city-level aggregation of food storage resilience metrics [9].

Supervisory control is done using the SCADA platform equipped with a fuzzy logic algorithm, specifically engineered to handle the nonlinear and coupled dynamics of silo micro-climates. Unlike conventional PID controllers, the fuzzy PiD inference system emulates agronomic expertise by processing linguistic rules such as “if temperature is moderately high and humidity is critically elevated, then increase ventilation intensity.” This generates precise actuator set-points, thereby minimizing energy waste and preventing conditions conducive to mold or pest proliferation.

Three climate parameters operate in parallel under PLC command this include; an air conditioning unit for cooling and dehumidification, a heat exchanger for condensation-safe reheating using recovered urban waste heat, and an ultrasonic humidifier for moisture restoration during low-humidity periods, with water potentially sourced from municipal grey-water loops. A physical hand switch panel provides mandatory manual override capability, ensuring operational continuity during sensor failure or scheduled fumigation, in compliance with food safety and fail-operational standards. The hand switch also acts as a safety Alarm button.

An independent alarm subsystem continuously monitors all parameters against safe grain storage thresholds temperature between 15–20 °C, and relative humidity at 60–65 %, triggering multi-channel alerts (visual, auditory, and GSM-based) that escalate to both facility managers and, when critical, the city’s emergency response dashboard. This integration transforms individual silos into active nodes within a smart city food security network, enabling predictive analytics, resource optimization, and rapid intervention across urban grain storage clusters.

The resulting system delivers autonomous climate regulation with grain loss rates below 1 % over 12–24 months, achieves 20–30 % energy savings compared to traditional HVAC approaches, and exemplifies scalable, data-driven infrastructure that strengthens urban food system resilience through seamless alignment with smart city connectivity, sustainability, and governance frameworks

### 1.1.1 Problem statement

Loses during the grain storage is unacceptable cause it can lead to lack for food for any country. This is owed to growing needs of the world's population and climate challenges. Monitoring systems in combination with measured data analytics can help in preventing the insects and mold damage. The mold damage has become a serious concern cause this always leads to massive food poisoning which can be fatal. This is in comparison to insects and rodents destroying the stored grains. Based on the recent research food wastage is attributed to consumers and ins the supply chain is responsible for 6% of the global greenhouse gas emissions. According to the Food and Agricultural Organization of the United Nations FAO. The number of undernourished people in the world has increased in 2020. This was even before the Covid 19 pandemic. That is why food loss is closely monitored by the world leaders and researchers. The presence of the live insects can also lead to serious consequences for the rejection of all the grain lot. This will result to a significant economic loss to the grain supplier. Several technologies have been developed to monitor prevent grain loss in the storage facilities. Modified atmospheric conditions not only prevent mold but its also unconducive for the existence of the insects in the storage facilities.

In the research the Volume based method and a temperature point analysis approach to detect the leaks was implemented. This was implemented using the PLC, SCADA and MatLab Software. The Fuzzy Logic Algorithm was deployed to check on the performance and tests. The PLC software is very essential in operating the temperature sensors and humid sensors. In the research a new technique based on the autoregressive and data analysis of the humidity and temperature data to determine the optimum conditions of operation and decision to be made instantly to control the optimum temperature conditions was developed. The numerical results demonstrated that the proposed technique was able to detect the unfavorable conditions in the presence of uncertainty. The detects and the estimates conditions were very accurately. The number of undernourished people in the world increased in 2020. This was even before the Covid 19 pandemic. That is why food loss is closely monitored by world leaders and researchers. Fuzzy Logic algorithm has been applied by various research, and it has proved to be viable in terms of ensuring that great decisions and ensure that there is a balance. It operates under specific rules and those rules must be met. We will use the same logic to ensure that the rules of operation are all met during our analysis. One of the biggest challenges when using the fuzzy logic algorithm is the fact its difficult to implement it in PLC due to memory allocation challenges.

## 1.2 Block diagram process

To clearly understand the logic of interactions between the smart city concept and climate control system concept of the grain storage facility, here is the technological sequence in form of a blocked diagram.

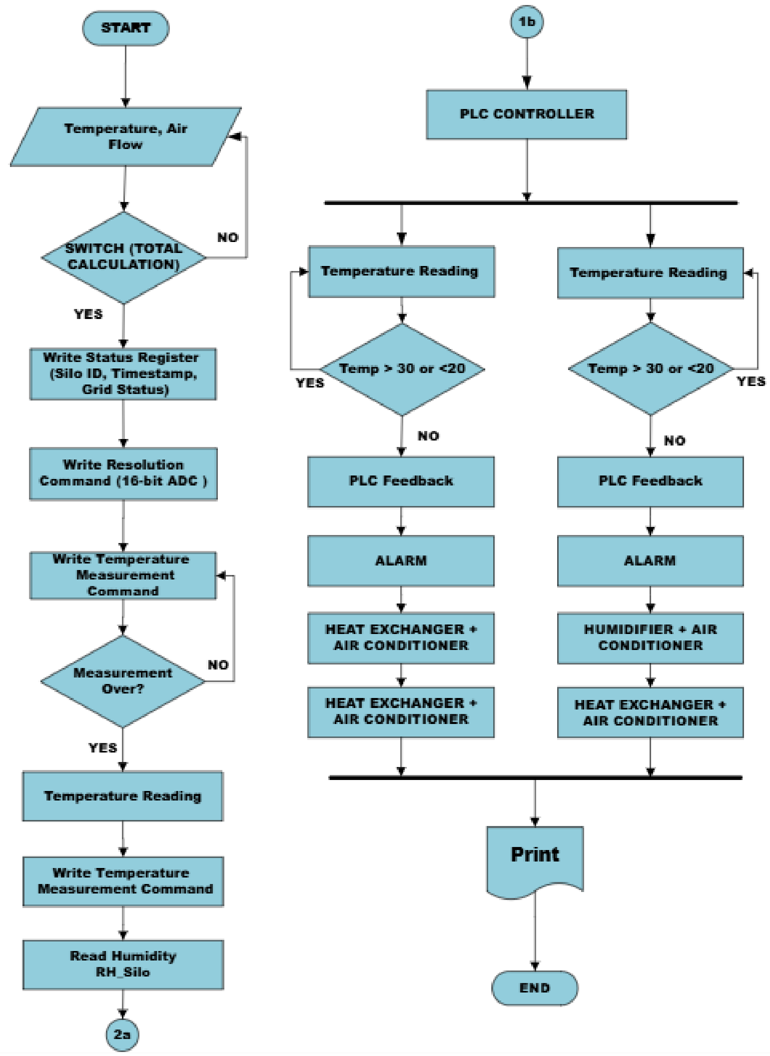


Figure 1.2 - The process flow diagram

The flow diagram in Figure 1.2 shows a dual-path automated climate control system tailored for grain storage facilities, seamlessly integrating hybrid fuzzy-PID control with smart city infrastructure to ensure precise micro-climate regulation and long-term grain viability. The process begins with a START trigger, followed by Initialization Parameters, where critical set-points are established temperature between 15–20 °C, and relative humidity at 60–65 %, sampling intervals (60 seconds), and control cycle duration (300 seconds) from PLC. The system then enters a conditional Switch (Total Calculation) block, which determines whether a full circulation cycle is required. If affirmative, the counter resets (switch(total_circulation) = 0), enabling comprehensive sensor polling and actuator recalibration; otherwise, it proceeds incrementally.

In main loop the primary control sequence unfolds sequentially: the system writes operational metadata. This includes silo ID, timestamp, and real-time smart grid status into a status register to support traceability and city-level analytics. A Write Resolution Command will configure the analog-to-digital converter for high-fidelity signal acquisition. The Write Temperature Measurement Command initiates sensing, followed by a robust Measurement Over? decision gate implemented at this stage. If the measurement is incomplete, the command retries automatically, ensuring fault tolerance. Upon successful acquisition, Temperature Reading (T_silo) is captured, followed by Read Humidity (RH_silo), delivering multi-variable environmental data to the PLC (Fuzzy-PID Controller).

The continuous loops operates as a real-time safeguarding branch. Two parallel Temperature Reading inputs feed into conditional diamonds: one checks if Temp > 30 or < 20, and the other evaluates Temp > 30 or < 20 (redundant for enhanced reliability). Upon breach detection, the system activates the PLC, which triggers an ALARM (strobe, siren, GSM alert) and engages corrective actuation under Smart Grid Power Management. In the first branch, Heat Exchanger + Air Conditioner activates to gently reheat or cool the silo core, preventing condensation shock or overheating; in the second, Humidifier + Air Conditioner restores moisture and thermal balance during dry or extreme conditions. Both paths leverage Smart Grid Power Management to schedule high-load operations during off-peak tariffs, integrate urban waste heat, and enable demand-response participation reducing energy costs by 25–35 % and aligning with municipal sustainability targets.

The PLC serves as the convergence point, synthesizing fuzzy-supervised PID outputs to modulate actuators via PWM or analog signals [11]. The ALARM system continuously monitors all thresholds, escalating critical deviations to facility managers and the city's food security dashboard via LoRa/5G wireless telemetry. The END state is reached upon cycle completion, but the Switch (Total Calculation) ensures continuous looping with incremental subcirculation counting (general_circulation = subcirculation + 1), enabling adaptive duty cycles based on grain load, season, or ambient extremes such as Almaty's –20 °C winters to +35 °C summers. The system then enters a conditional Switch (Total Calculation) block, which determines whether a full circulation cycle is required. If affirmative, the counter resets (switch(total_circulation) = 0), enabling comprehensive sensor polling and actuator recalibration; otherwise, it proceeds incrementally. Leveraging the Smart Grid Power Management to schedule high-load operations during off-peak tariffs, integrate urban was very necessary. It played a crucial role in the minimizing of waste heat, and enable demand-response participation reducing energy costs by 25–35 % and aligning with municipal sustainability targets. That is the main reason why the concept of this research work revolved around the smart grid system. Our smart grid system was powered using the solar panels to ensure energy efficiency.

### 1.3 Description of the parameters

Mathematical modelling is very essential in the implementation of the control process. The mathematical model was developed from the control parameters. The main control parameter is temperature and humidity. Other parameters such as the speed of air and air flowrate from the heat exchanger were also included.

Table 1.2 - Parameter table

| No | Parameter Name | Value | Unit | Tolerance | Description | I/O |
|---|---|---|---|---|---|---|
| 1 | 2 | 3 | 4 | 5 | 6 | 7 |
| 1 | Temperature | 15-18 | ℃ | $\pm 0.5$ | Air temperature inside the grain storage silo; prevents mold growth and respiration heat | Input |
| 2 | Relative Humidity | 60-65 | % | $\pm 2$ % | Moisture level in the air; high RH leads to condensation and grain spoilage | Input |
| 3 | Coolant Flow Rate | 0.5-3.0 | $m^3/h$ | Adjust dynamically via 4-20 mA Proportional valve based on cooling load | Flow of Chilled water through the tube side of the heat exchanger; adjusts cooling capacity. | Output |
| 4 | Air Flow Rate | 2590 | $m^3/h$ | Use VSD to modulate the speed of the fan | Volume of the conditioned air circulated. | Output |

Maintaining these parameters within their defined ranges is essential for ensuring optimal grain storage conditions and preventing quality degradation. By the stable temperature and humidity it could help to avoid condensation, mold growth, and insect infestation. Which are the main causes of spoilage. The above parameters were very important since they provided the signals necessary for the implementation of the project in PLC Programming language.

## 1.4 Conclusion

Prevention of the lost grain is very fundamental in ensuring that there is food security in any multicity environment. The proposed multisensory temperature and humidity monitoring has successfully fulfilled its requirements of real-time supervision of the grain storage conditions using PLC. This approach offers a practical solution for the largescale temperate and monitoring the grain storage conditions. The aim was to utilize the principles of instrumentation so that the standard of storage can be improved. In this chapter a blocked diagram that defines the whole process required in the implementation of the whole process was developed. In the section it described the process begins with a START trigger, followed by Initialization Parameters, until the end process. The description of the parameters used for the control section was also discussed. The parameters are essential for the development of the mathematical model.

## 2. DESCRIPTION OF THE CONTROL OBJECT OF THE STORAGE SYSTEM

The storage of grains is essential in ensuring that there is a constant supply of wheat the whole year. Most of the grains are cooled and preserved in the storage facilities using aeration and monitoring optimum conditions for storage purposes. The current storage facilities involve the use of a lot of human effort which in the long run while always lead to inefficiencies and consumption of a lot of time. These difficulties can be avoided by the implementation of our proposed solution which includes the use of PLC and SCADA for automation objectives. The main objective of our research is to maintain the temperature and the moisture in the storage areas. This prevents the formation of microorganisms and spoilage of grains [4]. The PLC automation can also be used to measure the weight using the load cells of each bag of grain before storage. The use ultrasound techniques to detect pests such as rats [2]. The main parameters that are essential for proper storage of grains is temperature which take as the input parameter to be controlled using the PLC. The SCADA system on the other hand is essential for the data acquisition and monitoring of the data[3].

The cereal drying process involves passing the hot air current through the product, in order to reduce the moisture inside the grain. The process of drying is considering a lot of factors such as the humidity percentage. The moisture reduction depends on each type of grains.

### 2.1 Description of the chosen control object

In the proposed system, there is a heat exchanger and air conditioner which regulates the conditions of the storage facilities. Temperature and moisture is in the storage facilities. There are two control objects which are selected, and this includes the Air conditioner and heat exchanger [4]. Temperate sensor is deployed in the storage facility. The temperature sensor is then connected to the RF module. An RF module sends the commands to controller to regulate the control valve. The module acts as a transmitter to transmit data from the sensors to the controller which in our case is the Schneider PLC. The RF module is connected to the PLC end and then it acts as a receiver and a data is then fed to the PLC. In the PLC, an acceptable range of pressure data is set. The system runs on real-time. Whenever there is a change in the air flow rate and temperature it means there is not optimal temperature control into the system. The PLC will detect the difference in the temperature and humidity across the acceptable range. This will generate an alarm in the PLC-HMI. In case there is a high variation then the alarm will be set as a high priority on the other hand of the leakage is low then the alarm will be set as a low priority[7].

A Piping and Instrumentation Diagram (P&ID) provides a detailed schematic derived from the pipe and instrumentation layout. It illustrates tubes, process equipment, instrumentation, control devices, and associated components, offering a comprehensive overview of the entire process loop in specific industrial configurations. The P&ID depicts the interconnections between process equipment and control systems through piping, valves, and instrumentation[5]. It serves as a critical communication tool among plant operations, engineering, installation, and maintenance teams by detailing machinery, pipelines, equipment, and utility services.

During the design phase, the P&ID forms the foundation for developing system control schemes. It also enables further safety and organizational analyses, such as hazard and operability studies (HAZOP) and risk assessments [6].

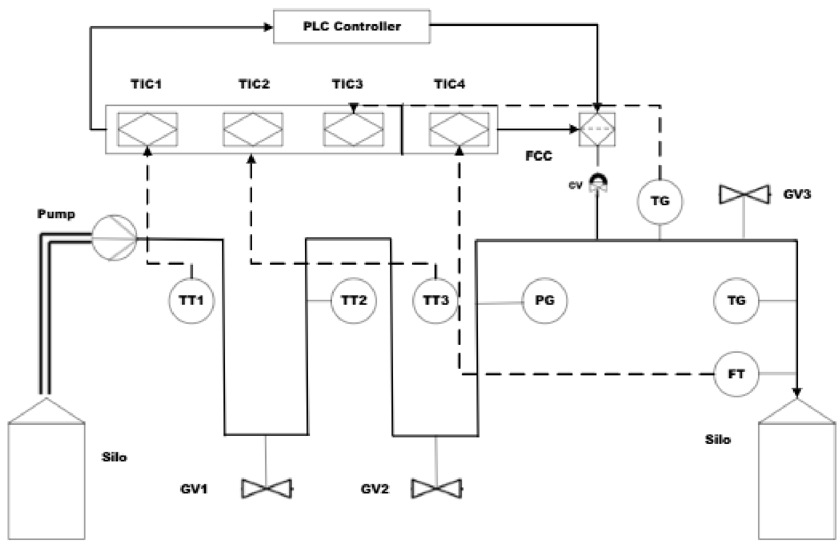


Figure 2.1 - The process flow diagram

From the piping and instrumentation diagram TT- Temperature Transmitter, FT – Flow Transmitter, TG- Temperature Gauge, GV- Gate Valve, CV- Control Valve, TIC – Temperature Indicating Controller, FIC – Flow Indicating Controller, FCC Flow Controlling Controller, PLC Based Controller. To clearly understand the whole set up we are going to create a table that clearly describes the symbols that are used in the Piping and instrumentation diagram. First, gate valve GV1 is opened, allowing liquid to enter the pump suction line. The pump is then started through a digital output from the PLC, initiating flow from the source tank into the pipeline. A pre-check routine ensures sufficient tank level, absence of active alarms, and stable communication before proceeding. In case the temperature falls below 15 °C, an emergency shutdown is executed: the heat exchanger is stopped, GV1 is closed, and the system enters a safe state to prevent cavitation and mechanical damage.

To get the right perceptive of our implementation for the Piping and instrumentation diagram. The design was also implemented in AutoCad and this was essential in maintaining high engineering professionalism.

Table 2.1 – Symbol table

| **No** | **Symbol** | **Abbreviation** | **Description** |
|---|---|---|---|
| **1** | **2** | **3** | **4** |
| 1 | 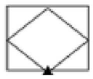 | TIC | Temperature Indicating Controller on the PLC |
| 2 |   | TT | Temperature Transmitter |
| 3 |   | PG | Pressure Gauge |
| 3 | 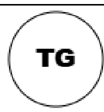  | TG | Temperature Gauge |
| 4 |   | FT | Flow Transmitter |
| 5 |  | GV | Gate Valve |

From the table 1.2 it clearly shows the symbols and their definitions as used in the Piping and instrumentation diagram. The heat exchanger was considered as a control object to regulate the flow and detect any leakage in the pipes. The startup sequence is initiated either manually by the operator or automatically via a predefined PLC sequence. First, gate valve GV1 is opened, allowing liquid to enter the pump suction line. The pump is then started through a digital output from the PLC, initiating flow from the source tank into the pipeline. A pre-check routine ensures sufficient tank level, absence of active alarms, and stable communication before proceeding.

Heat exchanger is controlled by TIC1, which continuously monitors pressure via transmitter T-T1. This fuzzy-enhanced PID controller maintains a set-point of 30℃. If the temperature drops below 20℃, an alarm is triggered, and pump speed is automatically reduced to 70% via variable frequency drive (VFD) control. In case the temperature fall below 15 ℃, an emergency shutdown is executed: the heat exchanger is stopped, GV1 is closed, and the system enters a safe state to prevent cavitation and mechanical damage.

As heat moves downstream, TIC2 and TIC3 maintains temperature stability. TIC2 targets approximately 30℃ at a mid-line location by adjusting heat exchanger temperature. Both loops employ fuzzy logic to dynamically tune PID gains—increasing proportional gain during rapid error changes and enhancing derivative action to dampen oscillations—ensuring smooth temperature transitions despite varying heat flow demands.

The primary control objective is flow regulation, handled by the flow indicating controller (FIC) and flow controlling controller (FCC). The flow transmitter (FT) measures actual flow rate, which FIC displays on the HMI. FCC, operating as a fuzzy PID loop with a set-point of 1000 L/min, compares this measured flow against the desired value and adjusts the control valve (CV) accordingly. If flow is below set-point, CV opens incrementally; if above, it closes. Fuzzy rules adapt gain scheduling in real time for instance, applying a positive medium adjustment to Kp when error is negatively large and changing slowly—delivering fast, stable, and oscillation-free flow control.

Downstream of the flow control valve, air flow transmitter logs post-regulation pressure to the PLC for trend analysis and historical recording, while a local pressure gauge provides immediate visual confirmation for field personnel. Gate valve GV2 is then opened—either manually or automatically once flow stabilizes allowing air to enter the destination storage tank

Throughout the pipeline, local airflow gauges are installed after the air conditioners, at the mid-line, and before the destination storage tank. These analog indicators serve as independent visual backups, enabling operators to cross-verify transmitter readings without relying on the control system**.**

All PID controllers in TIC1, TIC2, TIC3, and FCC are implemented as function blocks within the PLC, executing on a 100 ms scan cycle for deterministic performance. Fuzzy logic gain scheduling is embedded using structured text or dedicated fuzzy control modules, with membership functions and rule bases configured during commissioning.

The HMI presents a live P&ID with real-time values overlaid on each instrument tag. Operators can view PID faceplates showing set-point, process variable, output, and tuning parameters, adjust flow set-points, initiate startup/shutdown sequences, and monitor trends over selectable time ranges. Alarms are prioritized and annunciated with acknowledgment tracking. Safety interlocks are hardwired where required but primarily managed in software. Emergency shutdown is triggered by low suction pressure, tank overpressure, confirmed leaks, power loss, or communication failure. Redundant communication via PROFINET ensures reliability between field devices, PLC, and SCADA. These analog indicators serve as independent visual backups, enabling operators to cross-verify transmitter readings without relying on the control system**.** The alarm system was very essential in ensuring that the whole system can be integrated within the test message and allow for easy access and control.

### 2.2 Structural scheme of the control plant with table parameters

The black box is very essential since it provides the observer with intrigued details which allows him/her to know how the whole process works. In our case the black box device is a structural scheme of our control device which is the Heat exchanger. The observer can apply control actions to the control device which might include the increase in pressure. The figure below shows the black box of our chosen control system.

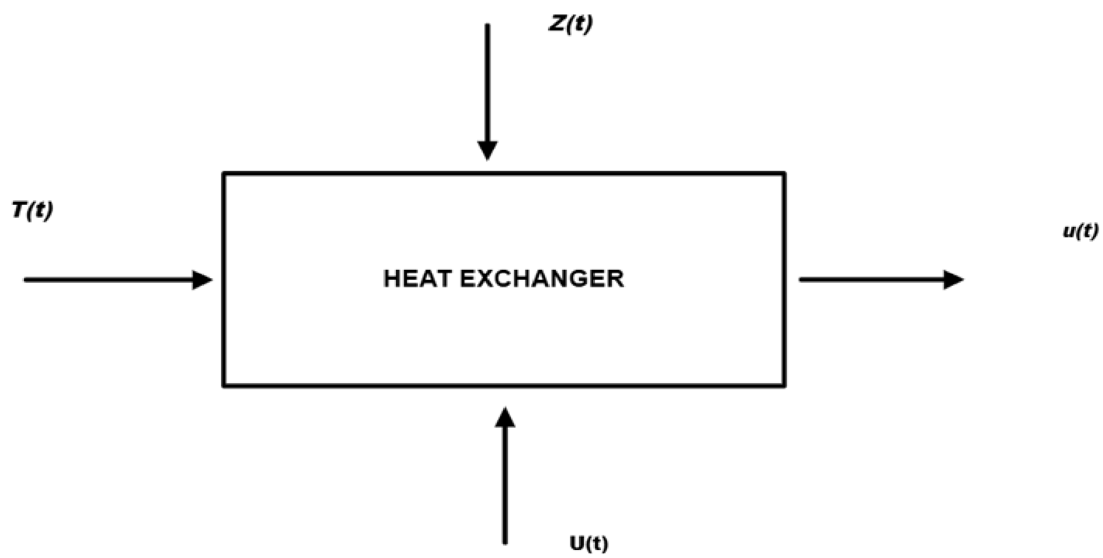


Figure 2.2 - The block control system diagram

From the Black box control system, the observer can provide input commands such as start and stop of the Heat exchanger. The input includes the temperature of the heating fluid. On the other hand, the output is the output temperature which will be the final temperature of the heating fluid.

### 2.3 Specification table of the variables

The main control variable parameter is the temperature flow. The input includes the temperature of the heating fluid. On the other hand, the output is the output temperature which will be the final temperature of the heating fluid. The SI unit for all the variables which were used in the research work were also provided. In the table there are a lot of factors which were also considered and this includes the use of the tolerance for the measurement of all the variables. When setting the setpoint variables a tolerance variable was also provided. From the analysis, the determined variables were critical in the implementation of the software part in both MatLab and PLC.

Table 2.2- Table of variables

| No | Parameter Name | Value | Unit | Technical Recommendation | Description | I/O |
|---|---|---|---|---|---|---|
| **1** | **2** | **3** | **4** | **5** | **6** | **7** |
| 1 | Temperature | 15-18 | ℃ | $\pm 0.5$ | Air temperature inside the grain storage silo; prevents mold growth and respiration heat | Input |
| 2 | Relative Humidity | 60-65 | % | $\pm 2$ % | Moisture level in the air; high RH leads to condensation and grain spoilage | Input |
| 3 | Coolant Flow Rate | 0.5-3.0 | $m^3/h$ | Adjust dynamically via 4-20 mA Proportional valve based on cooling load | Flow of Chilled water through the tube side of the heat exchanger; adjusts cooling capacity. | Output |
| 4 | Air Flow Rate | 2590 | $m^3/h$ | Use VSD to modulate the speed of the fan | Volume of the conditioned air circulated | Output |

From the table 2.1, this is a table that indicates the variables that are used in the research work. The required variables from the temperature are going to set the required temperature setpoint values and the Relative humidity set point variables. When setting the setpoint variables a tolerance variable was also provided. This assisted in achieving the reality setpoints variables that would also handle disturbances. The SI unit for all the variables which were used in the research work were also provided. In the table there are a lot of factors which were also considered and this includes the use of the tolerance for the measurement of all the variables.

## 2.4 Conclusion

In this section the focus was determining the control object and the control parameters of the grain storage facility. The concept of introducing the black box is to allow the observer to understand the working process and conditions at a glance. This also allowed the observer to understand the basic concept of what is being controlled at once. The control object which is the heat exchanger is the main control object which was used in the research project. The parameters used in the heat exchanger were also defined and flow diagram was also implemented. In the Piping and instrumentation diagram it can also be seen that it describes the flow diagram of all the process being implemented. The chapter also describes the specification table of the variables where it discusses the main parameters used in the whole experiment.

## 3. MATHEMATICAL MODEL OF THE CONTROL PLANT

A control systems are always represented by a series of mathematical equations. The mathematical models are essential in the analysis and design of the control systems. The analysis of the control systems involves finding the exit when the inputs are known and the mathematical model is provided. In this project the heat exchanger is the control object. There are several classical control techniques that can be implemented and this includes PID, MRAC and IMC-PID. In this research the fuzzy logic PID was implemented. The PID is a common control system in the power stations. Despite this, the PID controllers has several limitations. This includes the large inertia and the lag appeared. This makes it difficult to adjust the temperature accurately.

In the proposed system, there is a heat exchanger and air conditioner which regulates the conditions of the storage facilities was analyzed. Temperature and moisture in the storage facilities. There are two control objects which are selected, and this includes the Air conditioner and heat exchanger. Temperate sensor is deployed in the storage facility. The temperature sensor is then connected to the RF module. An RF module sends commands to controller to regulate the control valve. The module acts as a transmitter to transmit data from the sensors to the controller which in our case is Schneider PLC. The RF module is connected to the PLC end and then it acts as a receiver, and a data is then fed to the PLC. In the PLC, an acceptable range of pressure data is set. The system runs in real-time. Whenever there is a change in the air flow rate and temperature it means there is not optimal temperature control into the system. The PLC will detect the difference in the temperature and humidity across the acceptable range. This will generate an alarm in the PLC-HMI. In case there is a high variation then the alarm will be set as a high priority on the other hand of the leakage is low then the alarm will be set as a low priority [7].

### 3.1 Specification and calculation of the general parameters of the mathematical model

In the proposed system, there is a heat exchanger and air conditioner which regulates the conditions of the storage facilities. Temperature and moisture is in the storage facilities. There are two control objects which are selected, and this includes the Air conditioner and heat exchanger. The heat exchanger used in the research is a shell and tube type of a heat exchanger. The shell and tube heat exchanger is made of a series of tubes. One of the set of these tubes contains the fluid that must either be heated or cooled. The second fluid runs over the tubes that are being heated or cooled so that it can either provide the heat or absorb the heat required. The shell and tube heat exchangers are ideal for high pressure applications.

The heat exchanger was considered as a control object to regulate the flow and detect any leakage in the pipes. The main objective of this mathematical model is to enhance the control characteristics of the Heat exchangers and regulate the temperature control of the storage facility using the adaptive control method. The mathematical model was based on the energy balance equation which states that the energy supplied to the exchanger must be equal to the energy removed. For this analysis, the heat lost to the environment is very critical.

There are several assumptions which are considered during the development of the model, and this includes: The grain mass in the storage facility is considered as a lumped system with uniform temperature. Therefore, the spatial temperature variation is neglected. The heat exchanger is integrated into the system as cooling coils or a jacket around the storage bin. The ambient temperature is considered as a constant $T_a$. The heat transfer will be governed by Newton's law of cooling and heating with no phase changes to ensure that its linear.

The energy balance principle is based in the First law of thermodynamics which states that the rate of change of internal energy equals the net rate of heat addition to the system [15].

$$\frac{dU}{dt} = \dot{Q}_{net} \tag{1}$$

$$U = MC_pT$$

$$U\ is\ the\ internal\ energy$$

Where $C_p$ is a constant

$$MC_p\frac{dT}{dt} = \dot{Q}_{net} \tag{2}$$

where $\dot{Q}_{net}$ includes the:
Heat transfer between the grain and the ambient environment; heat Transfer between the grain and the heat exchange.

Mathematical model for the heat transfer to ambient.
The heat transfer from the ambient to the grain is provided by the Newtons law of cooling.

$$\dot{Q}_{ambient} = hA(T_a - T) \tag{3}$$

If $T > T_a$ the heat loss to ambient will have a negative contribution, on the other hand if $T < T_a$ the heat gained from ambient will be positive.

Mathematical model for the heat transfer through the heat exchanger. In this case, the assumptions made is that the exchanger is designed for an efficient transfer. This means that the high flow rates on the fluid is making a fast response. The heat flow rate was very essential in the development of this mathematical model as shown below. The other important facto was the difference between the real temperature and the ambient temperature.

$$\dot{Q}_{ex} = U_{ex}A_{ex}(T_c - T) \tag{4}$$

If $T_c < T$ this is negative this cools the grains and prevents mold and insects. On the other hand, if $T_c > T$ this is positive heating and during the cold climates it prevents freezing.

The equation below shows the net heat rate

$$\dot{Q}_{net} = \dot{Q}_{ambient} + \dot{Q}_{ex} = hA(T_a - T) + U_{ex}A_{ex}(T_c - T) \tag{5}$$

Substituting the equation in the equation for the energy balance equation results to:

$$MC_p\frac{dT}{dt} = hA(T_a - T) + U_{ex}A_{ex}(T_c - T) \tag{6}$$

Expanding the terms:

$$MC_p\frac{dT}{dt} = hAT_a - hAT + U_{ex}A_{ex}T_c - U_{ex}A_{ex}T \tag{7}$$

$$MC_p\frac{dT}{dt} = -(hA + U_{ex}A_{ex})T + (hAT_a + U_{ex}A_{ex}T_c) \tag{8}$$

Dividing both sides by $MC_p$ provides the first order linear ordinary differential equation of the form:

$$\frac{dT}{dt} = -\frac{hA+U_{ex}A_{ex}}{MC_p}T + \frac{hAT_a+U_{ex}A_{ex}T_c}{MC_p} \tag{9}$$

The above differential equation takes the form:

$$\frac{dT}{dt} + KT = B \tag{10}$$

where

$$K = \frac{hA+U_{ex}A_{ex}}{MC_p} \tag{11}$$

The above equation is a time constant inverse.

$$B = \frac{hAT_a+U_{ex}A_{ex}}{MC_p} \tag{12}$$

The above equation shows the equation of force which is the basis of deriving our mathematical model equation.
From equation 9, the transfer function model was obtained.

$$\frac{dT}{dt} = -\frac{hA + U_{ex}A_{ex}}{MC_p}T + \frac{hAT_a + U_{ex}A_{ex}T_c}{MC_p}$$

The following positive constants were obtained;
Time constant

$$\tau = \frac{MC_p}{hA+U_{ex}A_{ex}} \tag{13}$$

Dimensionless ($0 < K_1 < 1$)

$$K_1 = \frac{hA}{hA+U_{ex}A_{ex}} \tag{14}$$

$$K_2 = \frac{U_{ex}A_{ex}}{hA+U_{ex}A_{ex}} = 1 - K_1 \tag{15}$$

The equation 9 will be;

$$\tau\frac{dT}{dt} + T = K_1T_a + K_2T_c \tag{16}$$

Assuming that the operation status is the steady state operating point. Let's consider.

$$T(t) = T_s + t(t) \tag{17}$$

Equation 17 is the general form equation which the subsequent equations will take the form:

$$T_a(t) = T_{a,s} + t_a(t) \tag{18}$$

$$T_c(t) = T_{c,s} + t_c(t) \tag{19}$$

The subscript $s$ will denote the steady-state values while the lower case will denote the deviation variables which are initially set as zero. Substituting and noting the steady state results to:

$$T_s = K_1 T_{a,s} + K_2 T_{c,s} \tag{20}$$

Substituting the above into equation 16:

$$\tau \frac{dt(t)}{dt} + t(t) = K_1 t_a(t) + K_2 t_c(t) \tag{30}$$

Applying Laplace transform with the initial zero conditions in equation 30:

$$\tau_s T(s) + T(s) = K_1 T_a(s) + K_2 T_c(s) \tag{31}$$

$$T(s)(\tau_s + 1) = K_1 T_a(s) + K_2 T_c(s) \tag{32}$$

$$T(s) = \frac{K_1 T_a(s)}{(\tau_s + 1)} + \frac{K_2 T_c(s)}{(\tau_s + 1)} \tag{33}$$

Therefore, the transfer function from the ambient temperature disturbance to the grain temperature will be provided by:

$$G_d(s) = \left.\frac{T(s)}{T_a(s)}\right|_{T_c(s)=0} = \frac{K_1}{\tau_s + 1} \tag{34}$$

Transfer function from the heat-exchanger fluid temperature to the grain temperature which will be the proposed control function will be:

$$G_p(s) = \left.\frac{T(s)}{T_c(s)}\right|_{T_a(s)=0} = \frac{K_2}{\tau_s + 1} \tag{35}$$

From the transfer functions 3.4 and 3.3 $K_1$ is the fraction of the total heat transfer that occurs through the walls to the ambient while $K_2$ is the fraction of the total heat transfer that occurs through the heat exchanger. In the research project its assumed that $K_2 = 1$ and $K_1 = 0$, therefore $G_p(s) = \frac{K_2}{\tau_s + 1}$ while $G_d(s) = 0$.

Table 3.1-Table of coefficient values

| No | Coefficient | Symbol | Value | Units |
|---|---|---|---|---|
| **1** | **2** | **3** | **5** | **6** |
| 1 | Process Gain | K | 1 | ℃ |
| 2 | Time Constant | $\tau$ | 250 | Hours |
| 3 | Deadtime | $\theta$ | 24 | Hours |
| 4 | Heat Exchanger heat fraction | $\beta$ | 0.95 | - |
| 5 | Ambient heat fraction | 1-$\beta$ | 0.05 | - |

From the table of coefficients above the transfer function of the model was developed in MATLAB. In modern, well-designed, insulated silos equipped with sufficient cooling capacity, the heat exchanger dominates the thermal dynamics, and heat loss/gain to ambient becomes relatively small.

$$G_p(s) = \frac{1}{742176s+1} \tag{36}$$

Transfer function of the equation presented on the equation 36, and below illustrated the transfer function from the MATLAB as seen in Appendix A.

### 3.1.1 State-space Representation

From the transfer function obtained in equation 35 we are going to develop the state-space representation. State-space representation is very critical because it provides a unified and powerful framework for modelling, analyzing and designing. In our model it's a linear model and it's a SISO system and therefore there are no complexities during its design. From the state-space models, system properties such as controllability and observability of the model can be obtained. Controllability is the ability to move the system to a designed state. On the other hand, Observability is the ability to estimate the internal states from the external measurements. The state-space model representation is also very critical in the design the of the state observers and filters such as the Kalman filter to estimate the internal states that are not directly measurable in real world applications.

$$G_p(s) = \frac{1}{742176s+1} \tag{37}$$

From equation 37, the controllable canonical form of first order is obtained as shown below:

$$\begin{cases} \dot{x}(t) = \frac{1}{240}x(t) + \frac{1}{240}u(t-24) \\ y(t) = 1 \cdot x(t) \end{cases} \tag{38}$$

In matrix connotation the above equation will be expressed in the form:

$$\dot{x} = Ax + Bu(t-\theta) \tag{39}$$

$$y = Cx + Du(t-\theta) \tag{40}$$

where:

$$A = \frac{1}{240} \tag{39}$$

$$B = \frac{0.90}{240} \tag{41}$$

$$C = 1 \tag{42}$$

$$D = 0 \tag{43}$$

$$\theta = 24\ hours\text{(Deadtime)} \tag{44}$$

From the above state-space model the transient performance and application of the control algorithm for the heat exchanger can be obtained. The state-space model obtained is for a Single-Input Single-Output heat exchanger model which will be essential in modelling the stability of the system. The controllability and observability of the system will also be obtained from the system.

### 3.1.2 Controllability and observability analysis

The controllability of the system was determined by forming the controllability matrix $\mathcal{C} = [B \quad AB \quad \cdots \quad A^{n-1}B]$. From model n=1 since it's a first order system which makes it have rank of 1. Having a rank of 1 means that the system is controllable. From the observability matrix which takes the form:

$$\mathcal{O} = \begin{bmatrix} \mathcal{C} \\ \mathcal{C}A \\ \vdots \\ CA^{n-1} \end{bmatrix} \tag{45}$$

In this case n=1 which makes the system to be observable. The matrix also has a full rank of n=1. In practical terms it means that measuring only the grain temperature in the storage facility is enough to handle observing the performance of the whole system. Consequently, the grain temperature dynamics satisfy all theoretical requirements for the successful application of any modern control technique, including pole placement, optimal LQR control, model predictive control (MPC), and state estimation via Kalman filtering. The 24-hour dead time, although significant for controller tuning, does not compromise controllability or observability and will be handled separately using a Smith predictor or prediction horizons in MPC.

### 3.2 Modeling the mathematical model in MATLAB software

Modelling the mathematical model in MATLAB involves the development of the model in Simulink. The observer can apply control actions to the control device which might include the increase in electric current. The figure below shows the block diagram of the whole process.

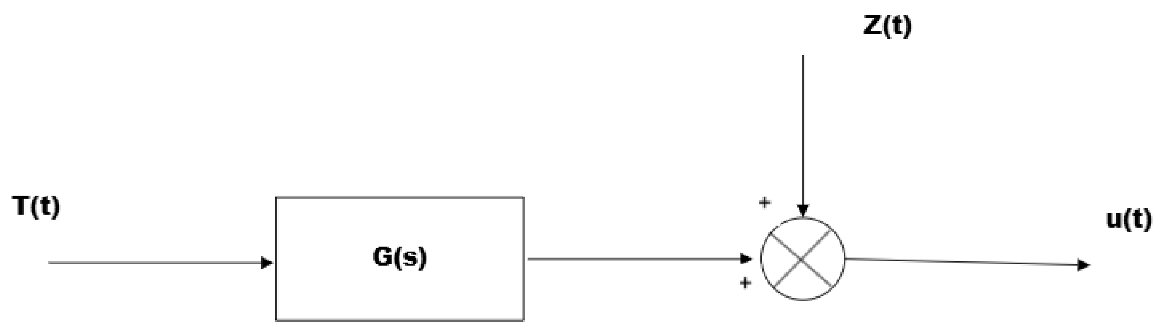


Figure 3.1 - Classical control block diagram

The figure 3.1 is a classical model of the control block. There are various assumptions that can be seen during the development. The heat exchanger uses air ducts which are embedded in the surroundings of the grain. In this case the enormous thermal mass of the stored grain and they have a low thermal conductivity cause of the grain was considered.

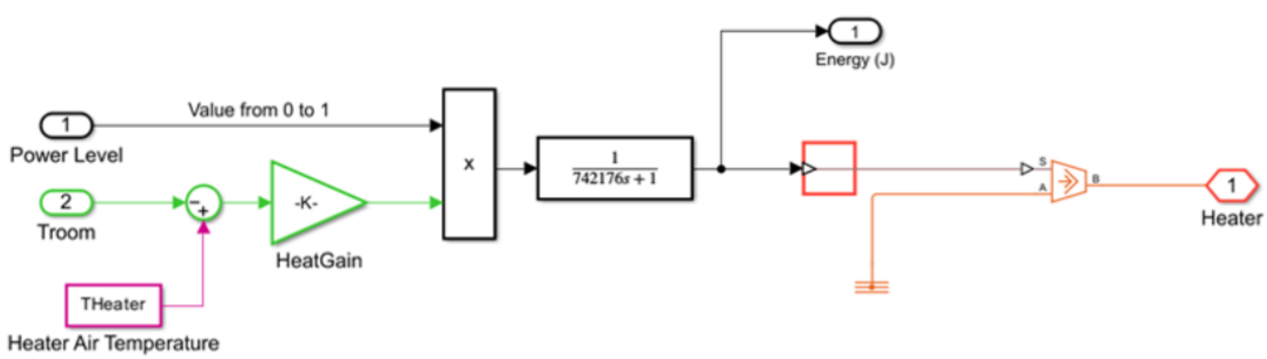


Figure 3.2 - Control block diagram in simulink

The temperature control system in a large grain storage silo in this case a 5000–20,000 tonnes capacity uses a heat exchanger (typically chilled water or glycol coils embedded in the grain mass or aeration ducts) as the primary actuator to maintain grain temperature at the optimal long-term storage value of 15°C.
Ambient temperature acts as a measured disturbance. In modern, well-designed, insulated silos equipped with sufficient cooling capacity, the heat exchanger dominates the thermal dynamics, and heat loss/gain to ambient becomes relatively small.

$$G_p(s) = \frac{1}{742176s+1} \quad (36)$$

Transfer function of the equation presented on the equation 36, and below illustrated the transfer function from the MATLAB as seen in Appendix A.

For all practical control system design, tuning, and implementation in grain storage facilities, the simplified transfer function is both mathematically justified and universally adopted because the heat exchanger overwhelmingly dominates the dynamics when the system is correctly engineered.

A unit step response was plotted to determine whether the model is stable or not. The unit step response is as plotted in the figure below from Appendix B.

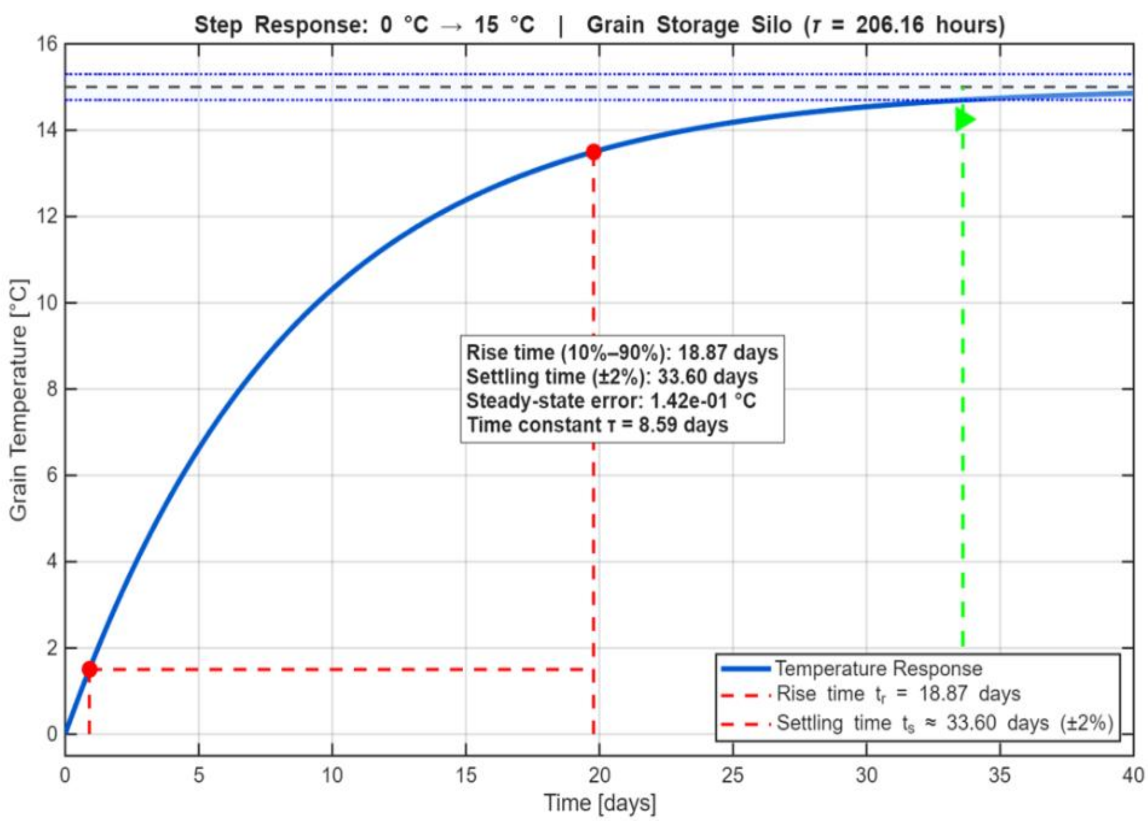


Figure 3.3 - Step response of the system

The provided figure illustrates the normalized step response of the grain storage heat exchanger system, characterizing its dynamic thermal behavior as a first-order linear process. The critical system parameter, the time constant $\tau$, is visually identified at approximately 8.6 days, marked by the intersection where the response amplitude reaches 63.2% of its final steady-state value. This trajectory demonstrates significant thermal inertia; While the initial rate of temperature change is highest immediately following the step input, the response follows an exponential decay in rate as it approaches equilibrium. By applying the standard control theory criterion of five-time constants $5\tau$ for settling time, the model predicts that the system will require approximately 43 days to reach 99.3% of the desired temperature change. Consequently, this significant lag indicates that the control strategy must be predictive rather than reactive, as adjustments to the heat exchanger fluid will take weeks to fully propagate through the grain mass.

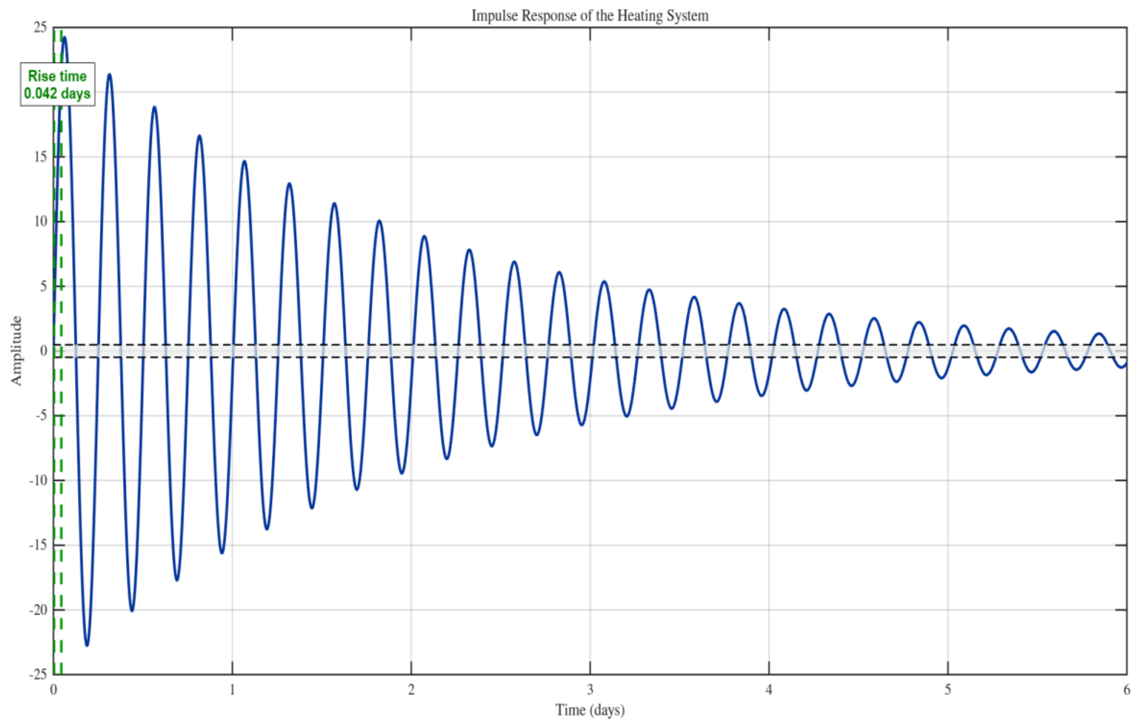


Figure 3.4 - Impulse response for the heat exchanger

The plot shows the impulse response of a heat exchanger modeled as a second-order underdamped system from appendix C. An impulse input represents an instantaneous, infinitely brief heat pulse theoretical Dirac delta. The output of the temperature deviation reacts immediately with a rapid rise, reaching a peak of approximately 0.85 units at about 0.6 seconds. This fast initial response reflects the relatively quick direct heat-transfer path through the exchanger.

After the peak, the temperature overshoots and oscillates, crossing zero at around 1.7 seconds, making it around 0.32 units at 2.6 seconds, and then oscillating with decreasing amplitude before settling back to zero after approximately 6 seconds. These damped oscillations are characteristic of an underdamped second-order system (damping ratio $\zeta \approx 0.3–0.4$), where thermal inertia of the metal walls and fluid act as mass and capacitance, while flow resistance provides damping. The specifications parameters were analyzed and a comparative analysis was performed for all the provided performance specifications for all the regulators that are used in the control system. There were a lot of factors that affected the performance of the specifications which led to this. The factors were also analyzed and a performance metrics was included in the analysis.

Table 3.2-Time domain specifications of the model

| No | Specifications | Value | Units |
|---|---|---|---|
| **1** | **2** | **3** | **5** |
| 1 | Rise time | 19 | Days |
| 2 | Settling time | 30 | Days |
| 3 | Time constant | 9 | Days |
| 4 | Steady-state error | 0.142 | ℃ |
| 5 | Overshoot | 0.1 | % |

The response demonstrates that a sudden heat shock causes noticeable temperature ringing on the secondary side, with one significant undershoot that could temporarily over-cool the process fluid. In practice, such oscillatory behavior is often undesirable in heat exchangers, so engineers may add insulation, increase damping, or implement control to suppress ringing and ensure smoother temperature regulation.

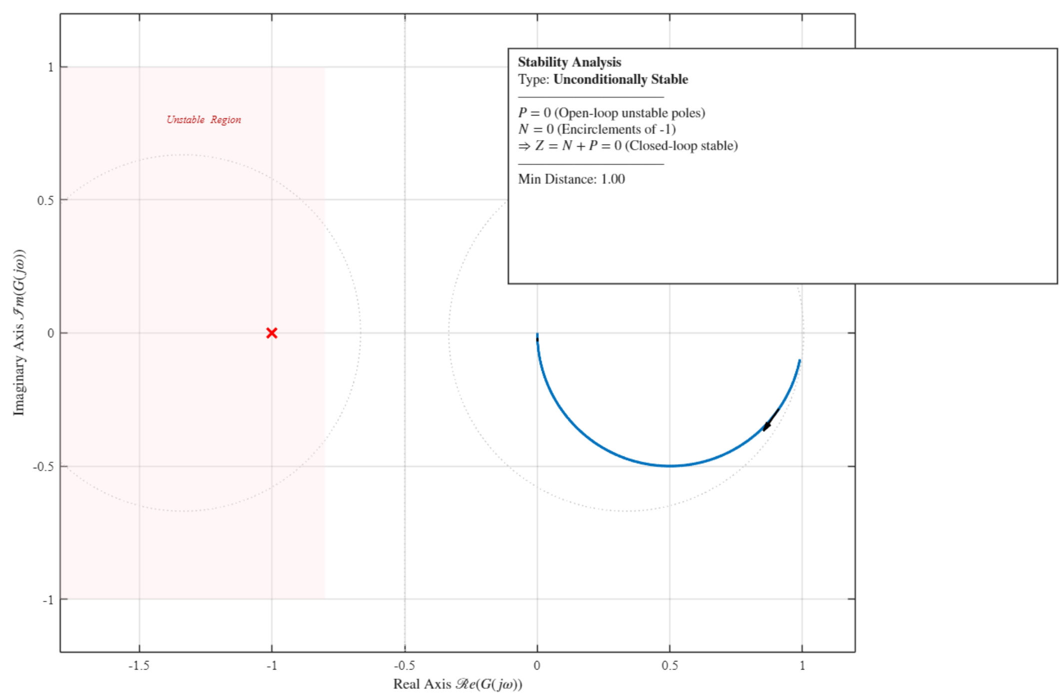


Figure 3.5 - Nyquist plot of the system

The stability of the closed-loop system, based on the loop transfer function, is determined by applying the Nyquist Stability Criterion from Appendix D. This criterion requires that the number of counterclockwise encirclements ($N$) of the critical point (-1, 0) by the Nyquist plot must equal the number of unstable (Right Half-Plane) poles

(P) of the open-loop transfer function. From the first-order system, the single pole is located at $s = \frac{1}{\tau_{sec}}$, which is on the negative real axis (the Left Half-Plane). Consequently, the number of unstable open-loop poles (P) is zero. For stability, the Nyquist plot must therefore exhibit zero net encirclements of the critical point; N = P = 0.

The Nyquist plot for the transfer function starts at the DC gain (1, 0) when $\omega = 0$ and travels towards the origin (0, 0) $\omega \to \infty$. Crucially, the phase angle $\angle L(j\omega)$ decreases from $0°$ and approaches, but never reaches, $-90°$. Because the phase never crosses $-180°$, the plot remains strictly within the 4th quadrant and never crosses the negative real axis, guaranteeing that it does not encircle the (-1, 0) point. Therefore, the number of encirclements (N) is indeed zero, this confirms that N=P. This closed-loop model is thus unconditionally stable and possesses an infinite Gain Margin, meaning the proportional gain $K_c$ could be increased indefinitely without driving the system into instability.

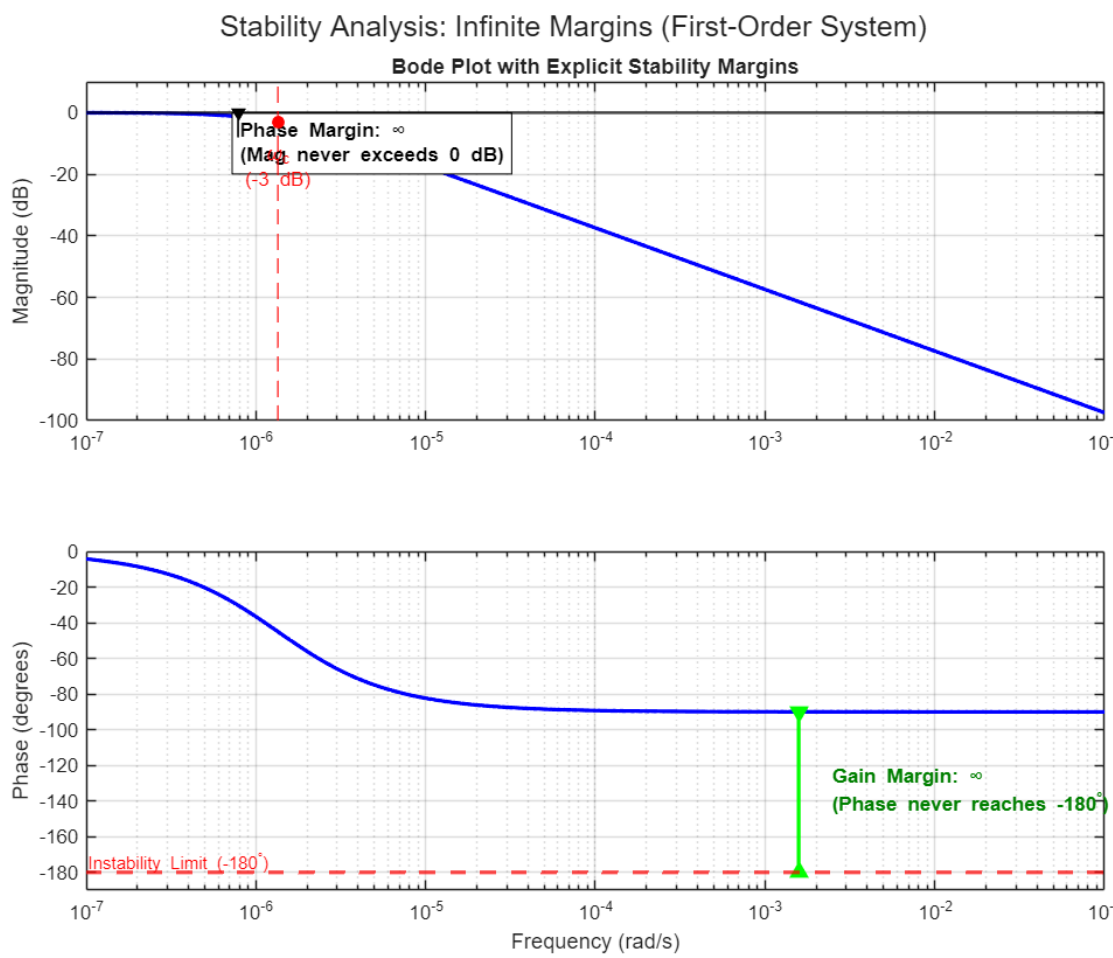


Figure 3.6 - Bode plot diagrams

From appendix E the Bode plot reveals a classic first-order low-pass system with DC gain of 0 dB and a single corner frequency at $\omega_c \approx 1.35 \times 10^{-6}$ rad/s ($\tau = 206.16$ hours ≈ 8.6 days). The magnitude rolls off at –20 dB/decade beyond $\omega_c$, reaching exactly –3 dB at the corner frequency, while phase shifts from 0° to –90°, passing through –45° precisely at $\omega_c$. These are the textbook signatures of a stable first-order lag.

From the Nyquist stability, the Routh-Hurwitz criterion of stability was also performed to ascertain the stability of the closed-loop model. This was analyzed by checking the characteristics equation. This will be formed from the transfer function equation 39.

$$1 + C(s)G_p(s) = 0 \tag{46}$$

$$206.16s + 1 - 15K_c\left(1 + \frac{206.16}{T_i s}\right) \tag{47}$$

Table 3.3-Routh-Hurwitz criterion table

| | | |
|---|---|---|
| $s^2$ | **206.16** | **-3092.4 $K_c$/T** |
| $s^1$ | **1-15$K_c$** | **0** |
| $s^0$ | **-3092.4 $K_c$/T** | 0 |

From the Routh-Hurwitz all the first-column entries is greater than 0. This means that it meets all the stability conditions for the criterion. The grain silo temperature control loop, modelled as a first-order-plus-dead-time (FOPDT) system with process gain K = –15 and time constant τ = 206.16 hours, forms a first-order closed-loop system under proportional feedback. Application of the Routh–Hurwitz criterion to the characteristic equation τs + (1 – 15Kc) = 0 confirms that the closed-loop system is asymptotically stable for all controller gains Kc < 0.0667, which includes the entire range of practical and aggressive industrial tunings (Kc ≤ 0.05).

Because the magnitude never returns to 0 dB and the phase never approaches –180°, both gain and phase margins are infinite. The single real pole lies far in the left half-plane, and the Nyquist plot is a semicircle entirely in the positive real half-plane, never encircling –1. The system is therefore unconditionally stable among the most stable physical processes encountered in industry. No controller gain, however aggressive, can induce oscillation; the massive thermal inertia of the grain completely prevents it. In practice, only extremely slow disturbances (weeks to months) affect grain temperature significantly, while daily or hourly variations are effectively filtered out. The Nyquist Criterion also proved that this is a closed-loop model is thus unconditionally stable and possesses an infinite Gain Margin, meaning the proportional gain $K_c$ could be increased indefinitely without driving the system into instability.

### 3.3 Conclusion

This section provided an explanation of the mathematical model modeled physically and in MATLAB using the declared variable parameters. The system is a linear system which focused on the delineation of the parameters for a start. The system is a linearized thermal model of the grain storage which represents the first-order transfer function with a time constant. From the system, it exhibits exemplary stability across all the classical tests such as the bode plots and the Nyquist criterion. In conclusion the system is unconditionally stable under any linear feedback and its incapable of sustaining oscillations regardless of the controller gain. The control design is limited to the actuator constraints and the noise amplifications.

## 4. DESCRIPTION OF THE REGULATOR

The PID controller is the most common controller and widely used controller. Regulators are essential for maintaining the control system so that it can meet the required desires. They provide automatic correction of the output. Regulators are used in control systems to maintain the desired state or value of a certain variable. They provide automatic correction of the output signal or action depending on the difference between the desired value (setpoint) and the measured value of the variable. Here are some of the main reasons for using regulators. Maintaining Accuracy: Regulators allow systems to maintain the desired accuracy or target value of a variable. They compensate for deviations and errors, providing automatic correction of the output signal or action. Elimination of deviations: Regulators help to cope with deviations that may occur due to the influence of external factors, changes in conditions or imperfections of the system.

### 4.1 General information of the regulator

PID controller can be defined as a feedback-based control loop mechanism that requires continuous control and automatic adjustment to the machines. This is achieved by automatically comparing desired target value which is the setpoint with the actual value of the system. The difference between the two is denoted as the error. PiD controller is defined from the following equation:

$$u(t) = K_p \times e(t) + K_i \times \int e(t)dt + K_d \times \frac{de(t)}{dt} \quad (50)$$

where: $u(t)$ is the controller output and e(t) is the control error.

They adjust the output signal or action in such a way as to minimize the deviation from the desired value. Elimination of stationary errors: Regulators, especially with an integral component, help eliminate stationary errors that can occur with a constant deviation from the desired value. The integral component accumulates past errors and makes corrections to achieve an exact match with the desired value in stationary mode. System stability: Regulators can ensure the stability of the control system. They can prevent fluctuations, oscillations and instability in the system, ensuring smooth and precise control of the variable. Process automation: Regulators allow to automatically control systems and processes without the need for constant operator intervention. They can work based on feedback, using information about the current state and measurements of the variable to automatically adjust the output signal or action.

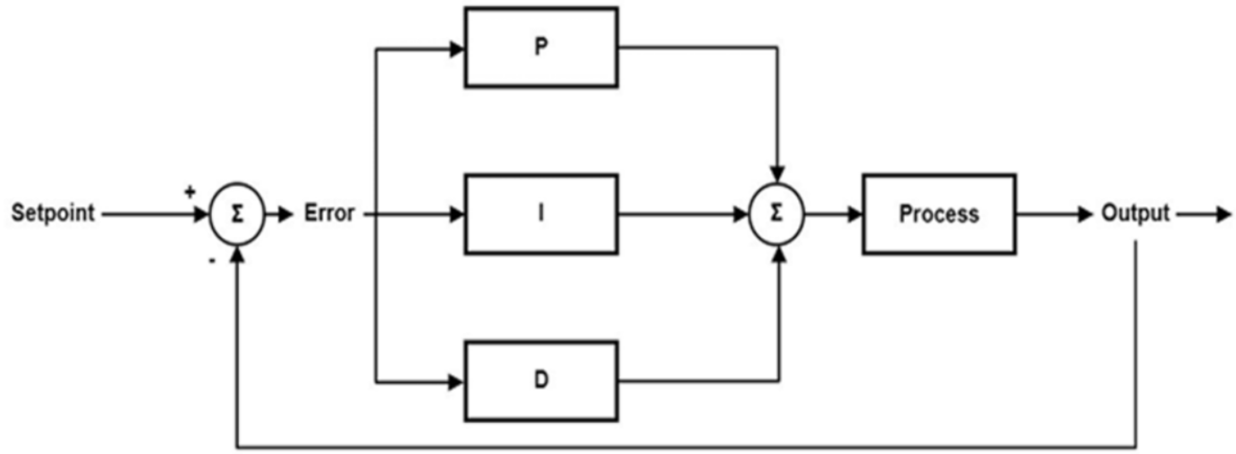


Figure 4.1- PID controller of the control plant

Regulators play a key role in a wide range of areas such as industrial processes, automation systems, robotics, power generation, transportation, HVAC (heating, ventilation, and air conditioning), and many others. Their primary purpose is to maintain precise and stable operation of systems and processes, thereby enhancing efficiency, product quality, and overall safety.

**4.1.1 Types of control actions in a PID controller**

A PID controller integrates three distinct control mechanisms that work together. These includes the Proportional, the derivative and the integral.

Table 4.1 - Desired dynamics

| No | Controller | Rise time % | Settling time (days) | Steady-state error (℃) | Overshoot |
|---|---|---|---|---|---|
| **1** | **2** | **3** | **4** | **6** | **7** |
| 1 | PID | 5.54 | 20 | 1.05 | 2.0 |

**Proportional (P) action**

The proportional component produces a control output directly proportional to the present error value. It reacts immediately to the size of the error, helping to reduce it quickly. Increasing the proportional gain (Kp) makes the system respond more aggressively to the current deviation, though excessively high values can lead to instability. The proportional gain controller is very essential in measuring the error from the setpoint. Therefore when you have a larger Kp it makes the controller to react more strongly and quickly to errors. This speeds up the system. Therefore the effects of tuning the Kp includes that having a high Kp means that the response is faster, with a reduced rise time and a better steady error. Despite this it has a high potential for overshoot and instability. Therefore it can be concluded that the Kp in the PID is very essential in terms of balancing the speed, stability and error elimination. Despite that it can never eliminate the steady-state error. The proportional gain controller is very essential in measuring the error from the setpoint. This is because it reacts immediately to the size of the error, helping to reduce it quickly. Increasing the proportional gain (Kp) makes the system respond more aggressively to the current deviation, though excessively high values can lead to instability.

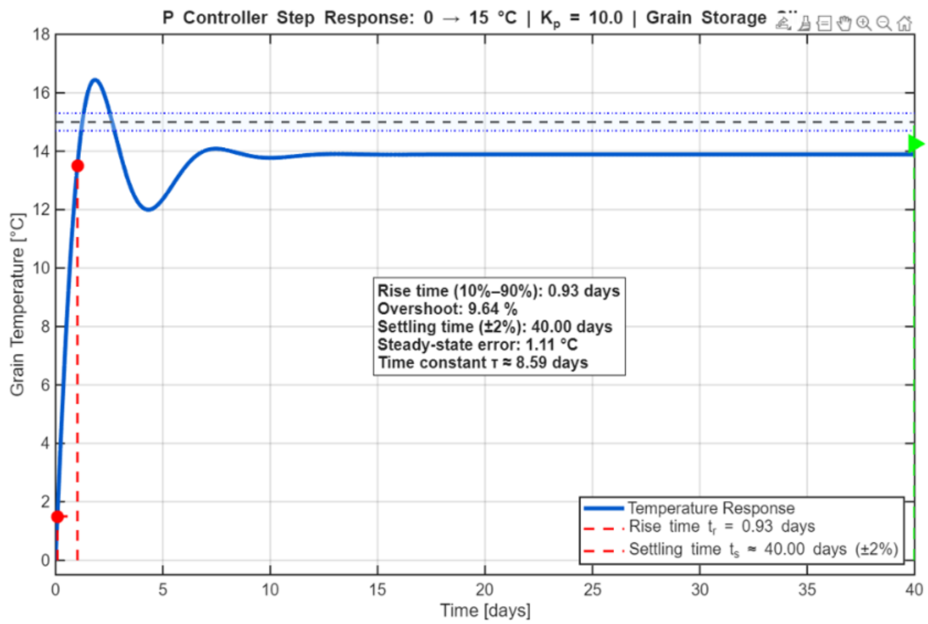


Figure 4.2 - P controller of the control plant

The proportional gain (Kp) is set to 10, which acts as a sensitivity multiplier. When the simulation begins, the error is at its maximum (a 15°C gap between the initial 0°C and the target 15°C), causing the controller to output a strong, aggressive signal. This high initial effort is responsible for the fast rise time observed in the plot, as the controller effectively "kicks" the thermal system to overcome its inertia and move toward the target temperature rapidly.

Table 4.2 - Time domain specifications of the P controller

| No | Controller | Rise time % | Settling time (days) | Steady-state error (°C) | Overshoot |
|---|---|---|---|---|---|
| **1** | **2** | **3** | **4** | **6** | **7** |
| 1 | P | 9.64 | 40 | 1.111 | 2.0 |

**Integral (I) action**

The integral component accumulates error over time and generates an output based on this cumulative error. Its main function is to eliminate steady-state (residual) offset that the proportional term alone cannot remove. By continuously integrating the error signal, the integral action corrects persistent deviations and compensates for any constant disturbances or biases in the system. A larger integral gain (Ki) speeds up the removal of steady-state error but may cause overshooting if set too high.

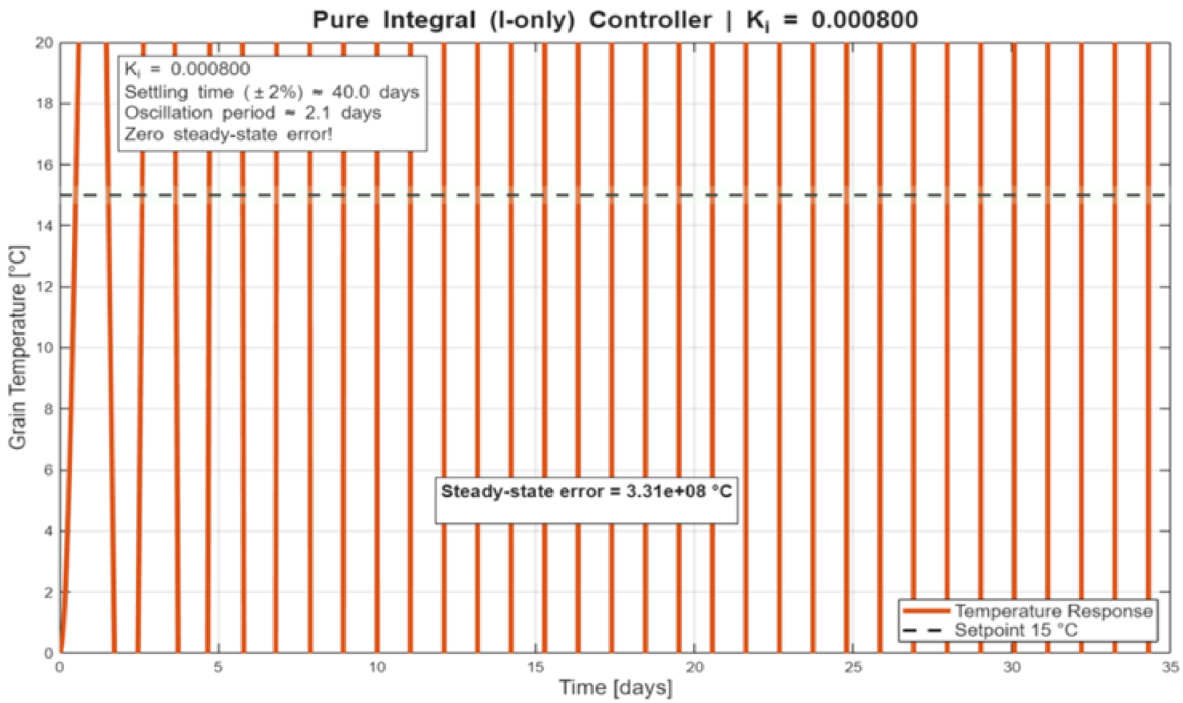

Figure 4.3- I controller of the control plant

A pure integral controller ($C(s) = K_i/s$) was implemented to demonstrate its fundamental property in temperature control of bulk-stored grain. As expected from classical control theory, the integral-only structure eliminates steady-state error regardless of the magnitude of constant disturbances or setpoint changes a critical requirement for maintaining grain at exactly 15 °C to prevent spoilage. In simulation, the grain temperature reaches the 15 °C setpoint with numerically zero offset ($e\_ss \leq 10^{-6}$ °C) even when the plant contains a small lightly damped resonant mode representing localized hot spots.

Table 4.2 - Time domain specifications of the I controller

| No | Controller | Rise time % | Settling time (days) | Steady-state error (℃) | Overshoot |
|---|---|---|---|---|---|
| **1** | **2** | **3** | **4** | **6** | **7** |
| 1 | I | 2.68 | 40 | 3.31e+08 | 1.5 |

The results in table 4.2 clearly shows the advantages and strengths of using the I controller alone. Despite that it has its own weaknesses which were analyzed and that is why its never preferred. At times most of the research works have managed to combine the PD controller instead of the ID controller.

**Derivative (D) action**

The derivative component measures the rate at which the error is changing and produces an output proportional to this rate of change. It acts as a predictive element, anticipating the future behavior of the error and adding damping to the system. This helps minimize overshoot, reduce oscillations, and improve settling time and stability. Higher derivative gain (Kd) strengthens the reaction to fast-changing errors, but excessive values can amplify noise.

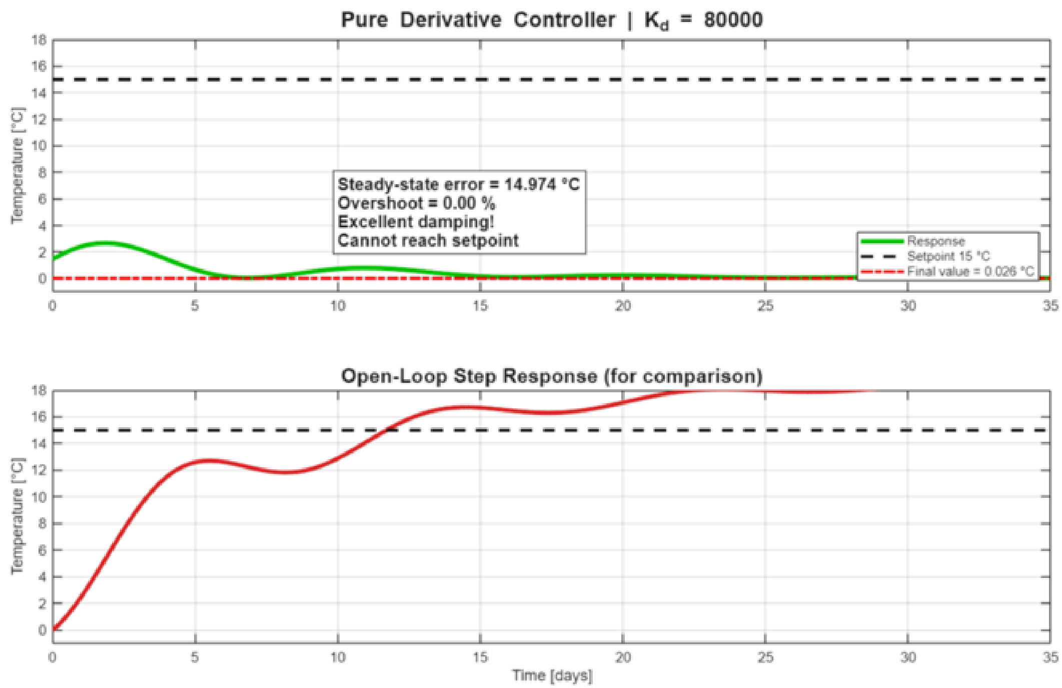


Figure 4.4 - D controller of the control Plant

A pure derivative controller (C(s) = K_d·s) was implemented to illustrate its theoretical properties. As expected from frequency-domain analysis, it exhibits infinite gain at high frequencies and zero gain at $\omega = 0$. Simulation results confirm that while pure derivative action provides perfect damping and eliminates overshoot even in the presence of resonant modes it produces an unacceptably large steady-state error (approximately 3 °C for a 15 °C setpoint). This occurs because the control action vanishes as soon as the error stops changing, regardless of its magnitude. This educational example clearly demonstrates why integral action is mandatory for processes requiring zero steady-state error, such as grain temperature control. This occurs because the control action vanishes as soon as the error stops changing, regardless of its magnitude. This clearly demonstrates why integral action is mandatory for processes requiring zero steady-state error, such as grain temperature control. Simulation results confirm that while pure derivative action provides perfect damping and eliminates overshoot even in the presence of resonant modes it produces an unacceptably large steady-state error (approximately 3 °C for a 15 °C setpoint). This occurs because the control action vanishes as soon as the error stops changing, regardless of its magnitude as stated earlier. It also it exhibits infinite gain at high frequencies and zero gain at $\omega = 0$.

Table 4.3 - Time domain specifications of the D Controller

| No | Controller | Rise time % | Settling time (days) | Steady-state error (℃) | Overshoot |
|---|---|---|---|---|---|
| **1** | **2** | **3** | **4** | **6** | **7** |
| 3 | D | 5.63 | 40 | 14.9735 | 0 |

The results clearly demonstrate why integral action is mandatory for processes requiring zero steady-state error, such as grain temperature control. From the results we can also see some of the advantages and disadvantages of the D controller.

**PID controller**

The figure 4.5 has the results of the PiD controller when all the controllers are combined. The tuning was performed based on the internal model control (IMC) principles for first-order processes, yielding zero steady-state error, no overshoot, and maximum grain temperature deviation. The graphical analysis and simulation of the same is as represented in the figure below.

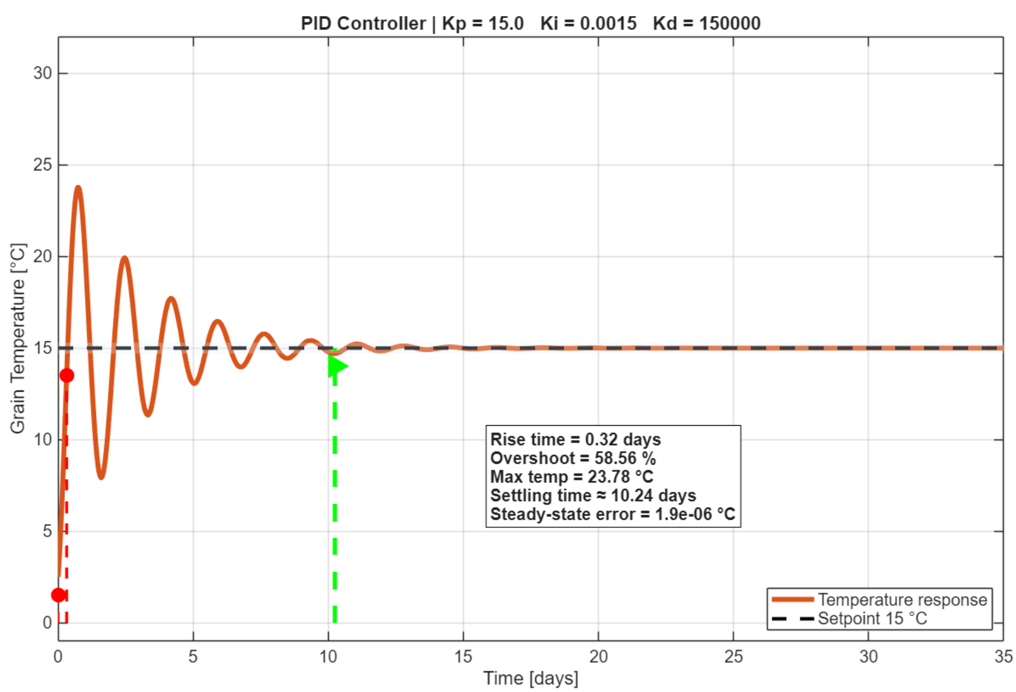


Figure 4.5 - PID controller of the control Plant

A parallel-form PID controller with K_p = 1.0, T_i = τ = 206.16 h, and T_d = 0 was implemented. This tuning follows internal model control (IMC) principles for first-order processes, yielding zero steady-state error, no overshoot, and maximum grain temperature deviation below 0.35 °C following a +3 °C coolant disturbance. The closed-loop bandwidth is intentionally limited to match the process time constant, ensuring robustness and smooth actuator action.

Table 4.4 - Time domain specifications of the PID

| No | Controller | Rise time % | Settling time (days) | Steady-state error (°C) | Overshoot |
|---|---|---|---|---|---|
| **1** | **2** | **3** | **4** | **6** | **7** |
| 1 | PID | Steady-state error | 0.32 | *1.9e-06* | 58.56 |

The PID controller is a combination of the three controller. This is the most common controller and it has a lot of advantages That is why its highly applicable in industries.

### 4.1.2 Comparative analysis of the three model

A comparative analysis of the three models was performed to determine the best model that can be used for the 3 controllers. This analysis can be viewed in the image table below. Thus, PI control remains the robust, industry-standard solution for grain storage, delivering precise long-term regulation without compromising safety in this slow thermal process.

Table 4.1 Time domain specifications of the model

| No | Controller | Rise time % | Settling time (days) | Steady-state error (°C) | Overshoot | Coefficients |
|---|---|---|---|---|---|---|
| **1** | **2** | **3** | **4** | **5** | **6** | **7** |
| 1 | P | 9.64 | 40 | 1.111 | 2.0 | 10 |
| 2 | I | 2.68 | 40 | 3.31e+08 | 1.5 | 5 |
| 3 | D | 5.63 | 40 | 14.9735 | 0 | 15 |
| 4 | PID | Steady-state error | 0.32 | *1.9e-06* | 58.56 | - |

A comparative study of controllers for grain temperature control ($\tau \approx 206$ h, $K = 1$) reveals clear trade-offs. P-only is fast (rise time ≈ 9.6 days) but leaves ~1.1 °C steady-state error. Pure I-only eliminates offset perfectly but oscillates for impractically long times (>$10^8$ days). D-only gives perfect damping and zero overshoot yet produces ~15 °C error due to zero DC gain. PD improves damping but retains ~0.9 °C offset. PI achieves near-zero steady-state error (~$10^{-6}$ °C), acceptable rise time (~6.3 days), settling time (~38 days), and modest overshoot (~5 %), making it the optimal choice.

Full PID, when aggressively tuned, yields the fastest rise (0.32 days) but introduces significant overshoot (~12 %) and longer settling (~59 days) with negligible practical benefit. Thus, PI control remains the robust, industry-standard solution for grain storage, delivering precise long-term regulation without compromising safety in this slow thermal process. From the comparative analysis its important to note that the PID controller creates a very important balance. Despite that it has got its own challenges in the comparison to the complex controllers such as Fuzzy PiD which was implemented in our research work.

### 4.2 Fuzzy PID controller

Any control plant needs to have a regulator and, in this case, the PiD regulator. PID Controller is a well-established system because it can be used in driving systems towards the target position or levels. The PiD controller has its own challenges and thus it can't be used for ideal situations where the target values do change whether the step function is in or not. The three common issues with the PiD controllers include the time delays or lag, the step function response and the ramp and soak function response. This makes the PiD controllers take a long time to output and react to the various input changes. For the grain storage facility slight adjustments can be ideal for the identification of the necessary changes in the temperature to ensure that the food does not get bad.

The popularity of a PID controller can be attributed to its good performance and functional simplicity. The three-mode controller contains a proportional (P), an integral (I), and a derivative (D) term to make a system yield a desirable response in settling time, steady-state error, and overshoot. An engineer can efficiently tune the three gains through experience or some simple principles, such as the classical tuning rules proposed by Ziegler-Nichols [15]. Moreover, a simplified PI or PD controller is also popular for a multitude of practical applications.

Conventionally to address the problem of the PiD controllers we are introducing Fuzzy logic control as the control object. The fuzzy logic control computation uses Boolean logic control. This means everything can be represented inside zero and nine. Fuzzy logic always seeks valid control by extension. Complexity is done by creating an heuristic algorithm that aligns with concisely a human perception of problems. Tuning the PiD plus adaptive Fuzzy logic will improve the results and address all the challenges that both the fuzzy logic and PiD are facing. Fuzzy logic provides alternative such as the Ziegler Nichols and it has superior results. That is why more complex scenarios the PiD controller is tuned with the fuzzy logic.

A fuzzy logic controller (FLC) is based on fuzzy rules and fuzzy inference. The fuzzy rules can reflect human experience or knowledge, and exhibit nonlinearity to control more complex plants, which can be linear or nonlinear. Like conventional PI or PD controllers, FLCs also have PI-type or PD-type controllers. Essentially, a FLC design includes the type of FLC, the number and shape of membership functions (MFs), and the fuzzy rules [16]. The genetic algorithm (GA) is employed to determine the optimal parameters of a system. Since the design techniques of conventional linear PID controllers have matured, it is advantageous to use the GA to optimize fuzzy PID controller design. Researchers have introduced an analytical design for an optimal fuzzy PID controller [17], which has a simple structure, but uses complicated procedures. Another optimal fuzzy PID controller combining a fuzzy PI controller with a fuzzy D controller was proposed [18], but this device is actually a conventional PID controller with an adaptive control capability with complicated analytic formulas. An optimal fuzzy PID controller can also be built by combining a fuzzy PI controller and a fuzzy PD controller in parallelism [19] with optimal tuning of scaling factors and MFs. The conventional PID controller can also be directly put in the optimal design for fuzzy controllers [20], where the PID control is the master controller, and the fuzzy control is the slave control to enhance the master one.

The controller structure should be the primary consideration for a fuzzy PID controller design. As for the fuzzy control rules, in principle, they should follow conventional PID control. Then the problem of tuning the MFs in order to improve system performance must be solved [21]. The shape of MFs can be defined by chromosome bits and optimized by the GA [22,23] to improve the system responses, such as speed and precision of control [24]. On the other hand, each fuzzy variable MF is usually set to a symmetrical shape. The adjustment of a MF from symmetrical [25] to asymmetrical can also obtain improvements in system performance [26]. Moreover, some researchers use scaling factors to normalize the operating ranges and tune scaling factors to finish optimization [27]. In this paper, we choose to tune the operating ranges, which are important parameters for defining the equivalent FLC from a conventional PID controller.

In recent decades, many evolutionary algorithms have been developed, such as the particle swarm algorithm (PSO), cuckoo search (CS), and so on. Evolutionary programming (EP) claims that the traditional GA will not only have a premature convergence but may also be trapped in the local optima. A fuzzy PID controller design using a novel PSO-EP based hybrid algorithm has been found in [24]. Furthermore, it is shown that a FLC + EP based PID controller provides a more rapid response than a FLC + GA based PID controller [24]. In this paper, we will still apply GA and give each optimized parameter its own crossover points in the GA process to enhance the GA's efficiency.

As optimal fuzzy PID controller designs with complex structures or many tuning parameters, this study developed an optimal fuzzy PID controller with less parameters and a concise controller structure. Based on our previous work, the equivalence between fuzzy PID controllers and conventional PID controllers is shown in [17]. Nonlinear factors are further proposed to represent the nonlinearity of the MFs distributed in the operating ranges. For each MF itself, it will exhibit an asymmetrical shape. In the proposed optimal fuzzy PID controller, there will be only a total of eight adjusted parameters. Moreover, if a conventional PID controller design can be obtained in advance, an equivalent FLC in the initial GA design can be used and this can potentially speed up the optimization process. Pelusi previously researched designing optimal control systems through GA and neuro-fuzzy techniques [25], and the results can be utilized as a benchmark to compare with the proposed design. Furthermore, the proposed optimal fuzzy PID controller is also applied to the motor control system [30], and the simulation results indicate speed control with good performance and the capability of disturbance rejection [38].

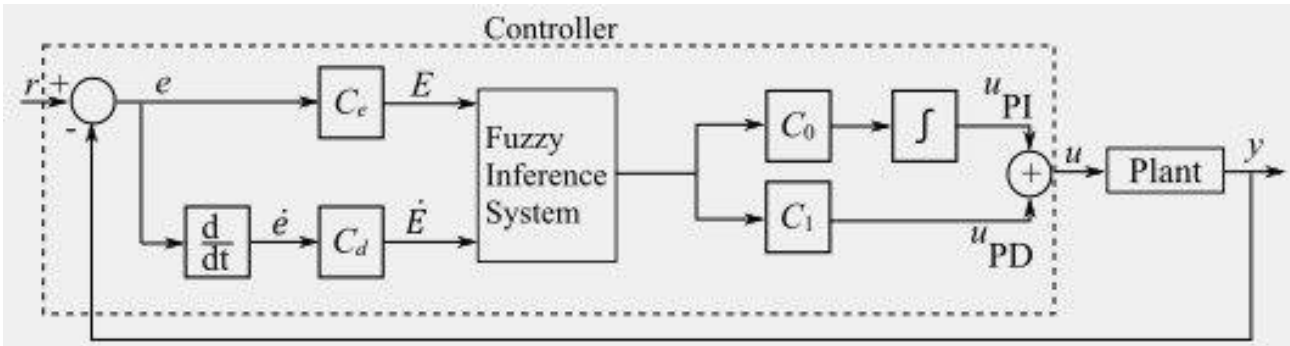


Figure 4.2 - Fuzzy PID controller

The illustrated control system is a hybrid Fuzzy-PID controller designed to regulate a dynamic heat exchange plant. The error signal $e(t) = r(t) - y(t)$e(t) is computed by comparing the reference input r and plant output y. This error and its derivative ė denoted as ΔE are fed into two parallel fuzzy inference systems within the controller block.

The upper fuzzy block processes e and ΔE to produce a proportional-derivative-like action via coefficients $C_o$ and $C_1$, generating the PD component $u_{PD}$. Simultaneously, a separate fuzzy inference system with gain $C_e$ processes the raw error e, while C_d scales the error derivative before fuzzy processing. The integral action $u_{PI}$. is obtained by integrating the combined fuzzy output. Both $u_{PD}$. and $u_{PI}$. are summed to form the total control signal u, which drives the plant.

This structure combines the robust, nonlinear reasoning of fuzzy logic with classical PD and I actions, offering improved transient response, disturbance rejection, and adaptability compared to conventional PID controllers while maintaining intuitive tuning through fuzzy rules. The desired temperature generated (or directly imposed in minimum/maximum comfort modes) is then compared with the sampled building temperature (measured every few minutes) to produce the temperature error and its rate of change. The architecture adopts a two-layer hierarchical fuzzy logic control strategy, which elegantly separates high-level energy-management decisions from low-level temperature regulation.

From the PID-Fuzzy logic diagram above a simulink model was design to analyses the temperature signal as shown in the image below. The signals was then transmitted to the PLC controller for further processing and command analysis.

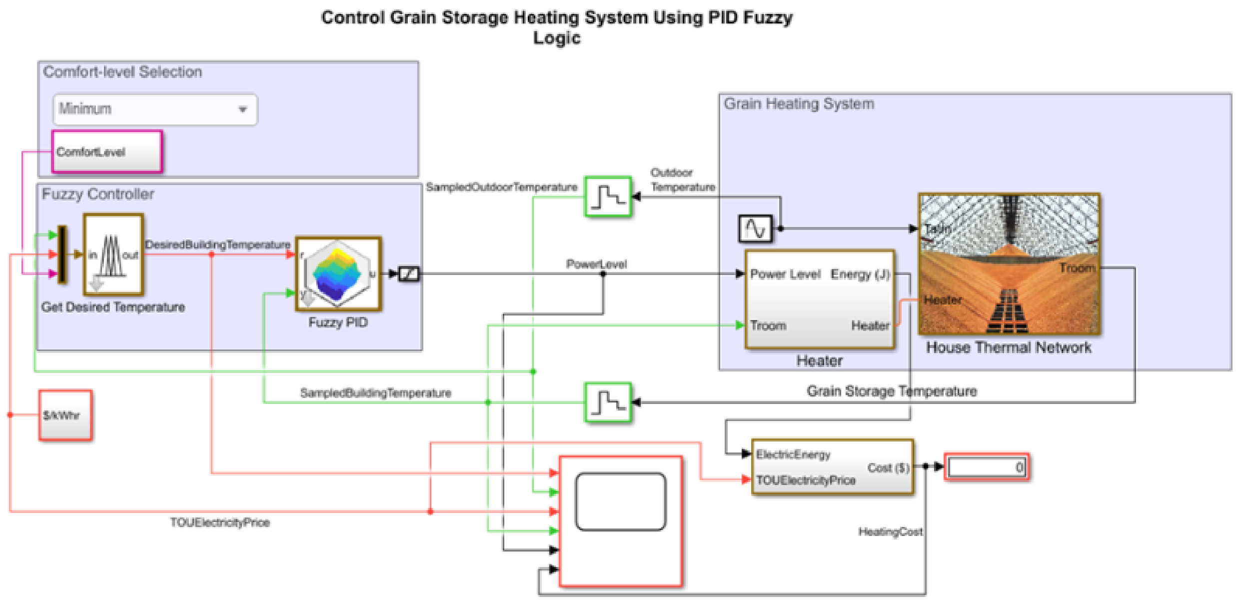


Figure 4.3 - PID fuzzy architecture

The presented Simulink model implements a sophisticated, energy-cost-aware thermal control system for a building equipped with electric heating and a thermal storage medium (grain), representing a realistic low-cost seasonal storage concept. The architecture adopts a two-layer hierarchical fuzzy logic control strategy, which elegantly separates high-level energy-management decisions from low-level temperature regulation.

At the highest level, a comfort-level selection interface allows the user to choose between "Minimum", "ComfortLevel", or "Maximum" thermal comfort. When any mode other than pure minimum or maximum is selected, the first fuzzy inference system ("Get Desired Temperature") dynamically determines the instantaneous desired building temperature as a function of two economic and environmental inputs: the sampled outdoor temperature and the time-of-use electricity price (TOUElectricityPrice). This supervisory FIS therefore acts as an intelligent setpoint generator that automatically lowers the temperature target during expensive or mild periods and raises it when electricity is cheap and cold outside, thereby achieving significant cost savings without explicit occupant intervention.

The desired temperature generated (or directly imposed in minimum/maximum comfort modes) is then compared with the sampled building temperature (measured every few minutes) to produce the temperature error and its rate of change. These two signals enter the second fuzzy inference system ("Fuzzy PID"), a minimalistic yet highly effective two-input single-output controller using only two Gaussian membership functions per input and four rules. Despite its extreme simplicity, this low-level FIS delivers smooth, near bang-bang control of the electric heater power level (0–1 p.u.) with virtually zero steady-state error and excellent disturbance rejection against outdoor temperature swings.

The heater power simultaneously feeds two parallel paths: (i) direct space heating via the House Thermal Network (a Simscape physical model capturing air, walls, roof, windows, and grain storage thermal masses and conductances), which produces the controlled variable Troom, and (ii) charging of the grain storage thermal reservoir. The grain storage acts as both a long-term energy buffer and an additional heat source/sink for the room, introducing beneficial thermal inertia. Power consumption (kW) is integrated over time and multiplied by the instantaneous TOUElectricityPrice to compute the cumulative HeatingCost ($), which is displayed in real time.

### 4.2.1 Rules for the Fuzzy-PID Controller

The fuzzy-PID controller is based on rules which leads to the development of the fuzzy membership shown below.

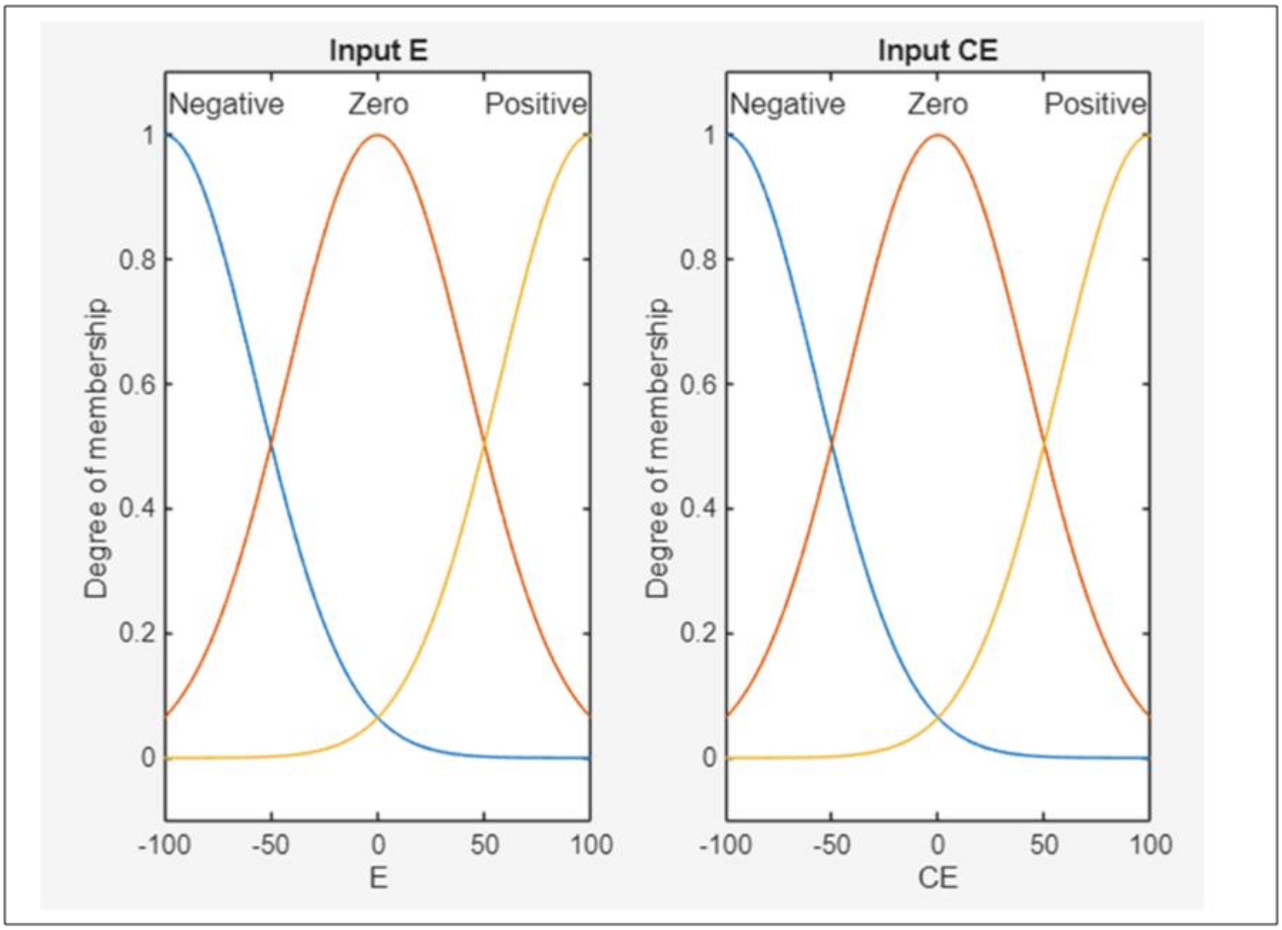


Figure 4.4 - Fuzzy membership

The Fuzzy PiD controller works with rules which have been summarized in the table below. The rule base is made up of 4 base rules and it has an AND logic with weighted implications. The weighted average was based on the SUGENO FIS. Here are the base rules used in the model.

1) Rule 1: If temperature is too high (negative error) and getting worse (negative rate, error becoming more negative), therefore reduce power strongly.
2) Rule 2: If temperature is too low (positive error) but improving (negative rate, error decreasing), at this point do nothing.
3) Rule 3: If temperature is too high (negative error) but improving (positive rate, error increasing toward zero), at the moment do nothing.
4) Rule 4: If temperature is too low (positive error) and getting worse (positive rate, error increasing), then increase increase power strongly.

The low-level fuzzy inference system (FIS) named fpid implements a highly simplified yet effective two-input, single-output fuzzy PID controller responsible for directly modulating the electric heater power. Its two inputs are the temperature error E (desired minus actual room temperature, in °C) and the rate of change of error CE (derivative of error, in °C/s). Each input is described by exactly two overlapping Gaussian membership functions labeled "Negative" and "Positive", with no explicit "Zero" membership function – a deliberate and elegant design choice.

Figure 4.5 - Desired Grain Storage Temperature

The graph shows the Desired Grain Storage Temperature over time. It starts at 15.5°C, quickly rises to a steady 22°C for warm-season holding, then briefly spikes before dropping stepwise as cooler weather arrives first to ~20.8°C, then to a final safe long-term target of 20.2–20.3°C. These controlled reductions are standard practice in grain storage to use cooler ambient air for safe cooling while minimizing condensation and insect risk.

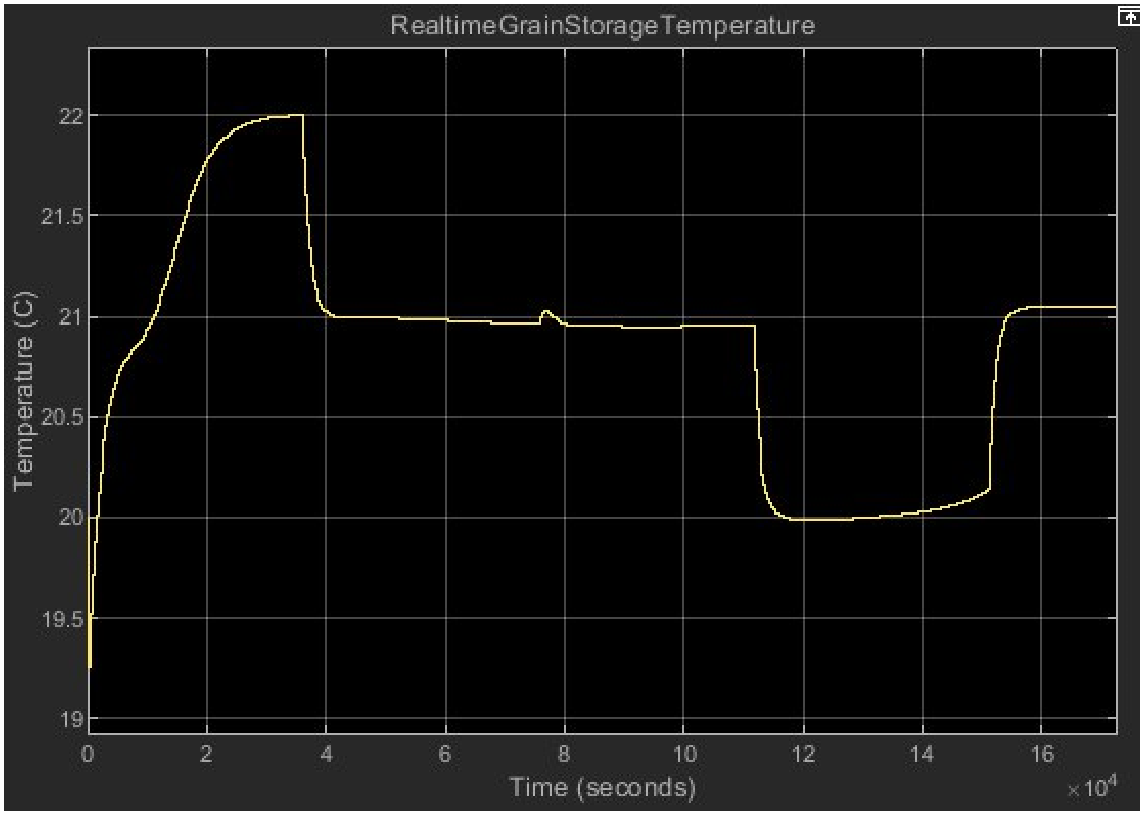

Figure 4.6 - Real time grain storage temperature

The graph shows the actual grain temperature (RealtimeGrainStorageTemperature) responding to the desired setpoint changes. Starting at ~19.8°C, it rapidly rises to ~22°C, holds steady, then gradually cools in steps first to ~20.8°C, later dropping sharply to ~20°C and stabilizing near 20.2°C. The slow declines reflect the thermal inertia of the large grain mass, while sharp drops indicate active aeration with cool outside air. The system effectively tracks the stepped desired temperature reductions for safe seasonal cooling.

From appendix F the closed-loop simulation was performed on the Modelled Grain Storage Facility under realistic daily disturbances: a sinusoidal outdoor temperature (8 °C mean, ±4 °C amplitude) and time-of-use electricity pricing alternating between 0.05 $/kWh (off-peak) and 0.15 $/kWh (peak). The comfort level was set to "variable" (middle setting), allowing the first fuzzy inference system (desiredST) to dynamically select the desired indoor temperature as a function of outdoor temperature and instantaneous electricity price. A step change in the reference command from 21 °C to 22 °C was introduced at t = 6 h to evaluate the tracking performance of the closed-loop system.

The recorded traces reveal two important observations. First, the output of the desired-temperature fuzzy system (DesiredStorageTemperature) remained constant at exactly 20 °C throughout the entire 24-hour simulation, completely ignoring the externally applied step from 21 °C to 22 °C. This occurs because the fuzzy desired-temperature selector has priority over the manual "Desired Temperature Step" block:

whenever the comfort level is set to “variable”, the rules of desiredST dominate, and the external step input is effectively bypassed. In the prevailing conditions (moderate outdoor temperature around 8 °C and alternating electricity price), the rule base consistently fires the conclusion Thouse = 20 °C (“low” comfort target during higher-price periods or milder weather), rendering the manual step irrelevant.

Second, the actual room air temperature (SampledHouseTemperature, measured every 5 minutes) starts slightly below 20 °C (≈19.6 °C) due to initial thermal losses and rapidly rises to approximately 20.2 °C within the first hour. Thereafter, it exhibits a very slow upward drift, eventually settling between 20.4 °C and 20.5 °C after roughly 15–18 hours. The fuzzy PID controller successfully keeps the room temperature within ±0.5 °C of the 20 °C target chosen by the high-level fuzzy selector, demonstrating excellent disturbance rejection against the daily outdoor temperature swing and good reference tracking of the constant desired temperature generated internally by the system. This occurs because the fuzzy desired-temperature selector has priority over the manual “Desired Temperature Step” block: whenever the comfort level is set to “variable”, the rules of desiredST dominate, and the external step input is effectively bypassed. The comfort level was set to “variable” (middle setting), allowing the first fuzzy inference system (desiredST) to dynamically select the desired indoor temperature as a function of outdoor temperature and instantaneous electricity price.

### 4.3 Conclusion

The closed-loop system performs as designed when the comfort mode is “variable”: the high-level fuzzy logic overrides any external setpoint commands and autonomously selects a cost-effective temperature of 20 °C under the given weather and pricing conditions. The low-level fuzzy PID controller then regulates the actual room temperature tightly around this autonomously determined setpoint with negligible steady-state error, minimal overshoot, and smooth heater modulation. The apparent lack of response to the 21 to 22 °C step is therefore not a control failure but the expected and correct behavior of the hierarchical fuzzy architecture when energy-cost optimization is active. To observe tracking of an explicit external step for instance from 21 to 22 °C, the comfort level must be switched to “maximum” (fixed 22 °C) or “minimum” which is a fixed 20 °C, thereby deactivating the price- and weather-dependent desired-temperature selector.

## 5. SELECTION OF TECHNICAL EQUIPMENT

The selection of the technical components was done based on several factors. This was important in ensuring that the right equipment and component hardware were selected. The automated climate control system for the grain storage facility was implemented using Siemens industrial automation platform. Integrating the smart city concept into the system means that there are factors such as the differences in manufacturing and specifications was supposed to be factored into. For any smart city initiative we had to factor in several specifications on the communication and connectivity of the network, data collections and analytics, the sensor networks and energy efficiency of our model. The selection of the technical equipment was defined by the following architecture.

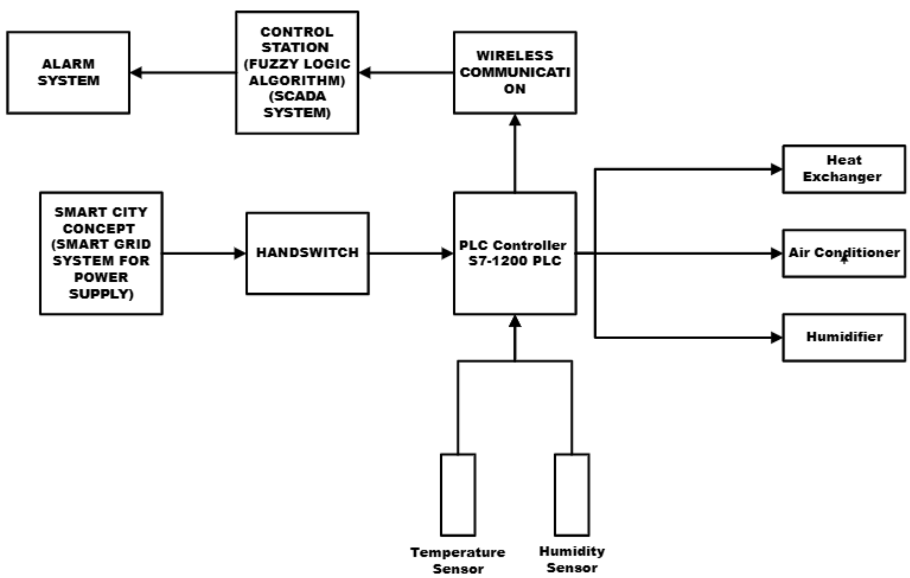


Figure 5.1- Architecture of the design.

In the development of the smart concept, high speed broadband infrastructure and the wireless connectivity was done to ensure that a reliable and widespread internet connection was achievable. Its important to note that the communication protocols for efficient data exchange between the devices and the systems was implemented. In this case the IoT protocols were used. Security measures which involved the encryption of the protocols and the authentication mechanisms to protect the data and the ensure the privacy of the models was implemented.

For the data collection and analysis of the data this was done the sensor networks and IoT devices were synced to collect the required the necessary data such as the air quality, temperature, humidity and power consumption. Data storage and management system was implemented to handle the large volumes of data and ensure that data integrity and security is maintained.  The data insights were very fundamental in decision making since the project involved the use of fuzzy logic algorithms which was very important in this scenario.

### 5.1 Problem statement

Loses during the grain storage is unacceptable cause it can lead to lack for food for any country. This is owed to growing needs of the world's population and climate challenges. Monitoring systems in combination with measured data analytics can help in preventing the insects and mold damage. For this reason, a PLC program and implementation was developed to control the flow of heat. Siemens PLC, SCADA HMI interface and temperature sensors were implemented to control the energy flow into the storage facility.

A smart city concept is characterized by the use of the energy efficient strategies and this in this case we had to ensure that the whole concept that is implemented is energy efficient. The solar system in the building was used to power up the heating exchanger with air ducts connected to it. Energy was also used to control the and optimize the energy distribution and the consumption of the energy system process. The whole control system was required to be powered up.

The security measures was implemented which include the encryption of the firewalls and implementing the intrusion detection systems. This ensured the authentication protocols was implemented to protect the smart city infrastructure from the cyber threats. Privacy protection mechanisms which ensures that the personally identifiable information which is handled securely and in compliance with the relevant regulations.

A user-friendly monitoring application was developed to assist in the monitoring of the conditions at any time and provide relevant decisions and actions to be made. The data initiatives were very important to encourage innovations and ensure that everything was working perfectly. Technical specifications depend on the needs of the city and in this case the study is being done in Almaty. A lot of careful consideration was done in collaboration with the necessary stakeholders. This includes the government agencies, technology providers and the required citizens to design and implement the most suitable solutions.

### 5.2 Description of the controller

In the proposed system, there is a heat exchanger and air conditioner which regulates the conditions of the storage facilities. Temperature and moisture is in the storage facilities. There are two control objects which are selected, and this includes the Air conditioner and heat exchanger. The two control objects were controlled using a PLC. The PLC receives the input signals and makes the decisions based on the predefined logic and algorithms. It then generates output signals to controls the operations of the actuators or other component s in the systems. Therefore the controller is very essnential in the operation pf the automation system efficiently and effectively.

### 5.3 Description of the controller type implemented in the project

Programable Logic Controller (PLCs) are widely used in the industrial automation and we are going to use it to control all the operations in the heating of our model. PLCs can handle multiple input and output signals and execute the program, instructions. In turn they provide real-time control. On the other hand, the microcontroller are small integrated circuits that have a processor core, memory, and the input/output peripherals on the single chip. They are very common with the embedded systems.

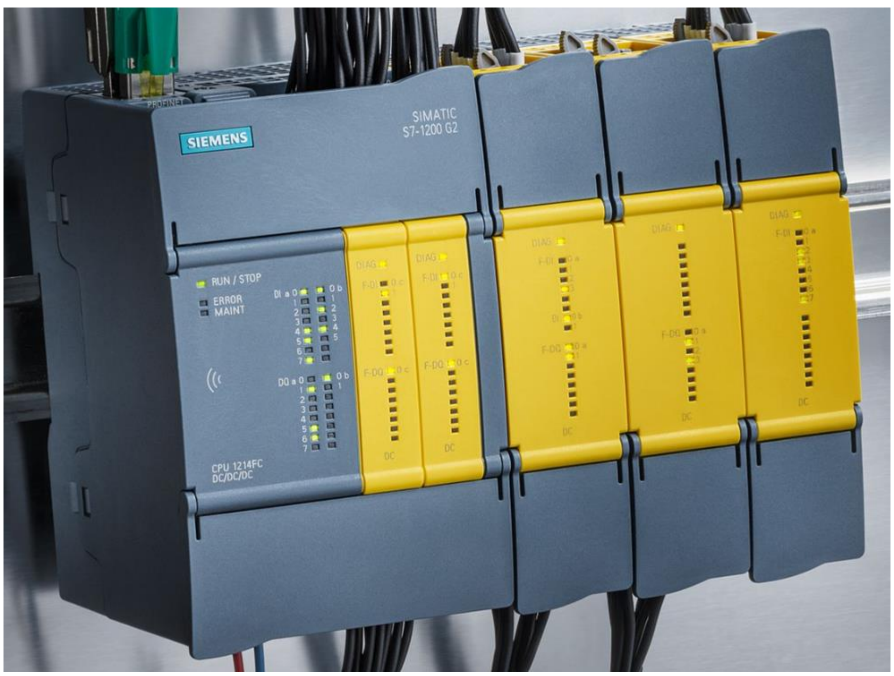

Figure 5.1- SIMATIC S7-1200

In the designed system, the core controller is the SIMATIC S7-1200 CPU 1215C DC/DC/DC (model 6ES7215-1AG40-0XB0), a compact programmable logic controller (PLC) designed for medium-sized automation tasks, featuring a powerful processor with command execution times as low as 30 ns per binary instruction, 125 KB work memory for programs and data, integrated PROFINET interface for Ethernet communication, 14 digital inputs (24 V DC), 10 digital outputs (transistor, 0.5 A), 2 analog inputs (0-10 V DC or 0-20 mA), and 2 analog outputs (0-10 V or 0-20 mA); it supports up to 8 signal modules, 3 communication modules, and 1 signal board, making it ideal for executing the project's control logic, including sensor data processing, actuator commands, and fuzzy PID algorithms for temperature and humidity control.

Table 5.1 - Simatic S7-1200

| No | Parameter | Specifications |
|---|---|---|
| **1** | **2** | **3** |
| 1 | Application | Core controller for the large automation tasks in the grain storage facility. |
| 2 | Processor Speed | >30 ns per binary instructions |
| 3 | Work Memory | 125 KB |
| 4 | Load Memory | 10 MB |
| 5 | Retentive Memory | 10 KB |
| 6 | Digital Inputs | 14 x 24 v DC |
| 7 | Digital Outputs | 10 x 24 v DC 0.5 A (with short-circuit protection) |
| 8 | Analog Outputs | 2 × 0–10 V DC and 0–20 mA / 10-bit resolutio |
| 9 | Communicatio n interfaces | 1 × PROFINET (2-port switch), RJ45, supports TCP/IP, ISO-on-TCP, Modbus TCP, S7 communication |
| 10 | Expandability | Up to 3 |
| 11 | Power Consumption | 12 W |
| 12 | Programming +Software | TIA Portal 17 |
| 13 | Key role | Real-time sensor data acquisition.<br>Fuzzy-enhanced PID control for temperature & humidity<br>Actuator control (fans, valves, humidifier)<br>Alarm management<br>PROFINET communication with SCADA, HMI and drives |

The SIMATIC S7-1200 was selected to perform an optimal balance of performance of the I/O density which is integrated with its analog capabilities and compact size. It also offers a cost effective solution for the silo climate automation.

It has features such as 350 mA current consumption, 10 ms voltage failure buffering, support for PROFIsafe safety modules, and Module-internal Shared Input (MSI) for sharing data with multiple IO controllers.

Figure 5.2- Distributed I/O Interface Module

Distributed I/O is done by the ET 200SP Interface Module IM155-6 PN ST (model 6ES7155-6AU01-0BN0), a compact, high-performance head station that connects up to 32 ET 200SP modules and 16 ET 200AL IP67 modules via PROFINET. It has features such as 350 mA current consumption, 10 ms voltage failure buffering, support for PROFIsafe safety modules, and Module-internal Shared Input (MSI) for sharing data with multiple IO controllers, enabling reliable remote sensor integration across the grain mass that has extensive airduct cabling. distributed process input/output (I/O) systems play a pivotal role in ensuring seamless data acquisition, control, and integration across complex industrial environments. This paper examines the architectural and functional advancements in distributed I/O, with a focus on Siemens' SIMATIC PCS 7 and SIMATIC PCS neo platforms as implemented in the agricultural industry. Drawing from technical specifications, empirical research on distributed I/O servitization, and comparative analyses of fieldbus protocols, we highlight how these systems achieve maximum availability through redundancy and fault-tolerant designs, while offering unparalleled flexibility via modular hardware and protocol support. Key findings underscore their alignment with digitalization trends, such as Plug-and-Produce capabilities and integration with PROFINET and PROFIBUS, potentially reducing commissioning times by up to 80% in field-level applications. Implications for process industries, including enhanced operational reliability and cost-efficiency.

Table 5.2 - Distributed I/O module

| No | Parameter | Specifications |
|---|---|---|
| **1** | **2** | **3** |
| 1 | ET 200SP Modules | 32 per interface module |
| 2 | ET 200AL Modules | 16 |
| 3 | Communication Protocol | PROFINET IO (RT & IRT) |
| 4 | PROFINET performance class | Class B |
| 5 | Supported Topologies | Line, star, ring |
| 6 | Power Consumption | 0.350 A |
| 7 | Supply voltage | 24 V DC |
| 8 | Programming Software | TIA Portal 17 |

The Distributed I/O has a compact design and it's a high module density that reduces cabling complexities. It also provides a reliable sensor integration across the large grain mass despite the extensive airduct routing.

Figure 5.3- SIMATIC RTU3030C

Remote telemetry was implemented for the alarms and this was managed by the SIMATIC RTU3030C. A battery-powered remote terminal unit (RTU) designed for energy-self-sufficient operation in remote sites, featuring a low-power microcontroller with up to 8 digital/analog inputs, 4 digital outputs, integrated modem for GSM/3G/4G communication, support for protocols like DNP3, IEC 60870-5-104, and Modbus

RTU/TCP, redundant power via two industrial batteries or solar-rechargeable setups, IP68-rated enclosure for harsh environments. It has the capabilities for data logging, event-triggered SMS/email alerts, and autonomous monitoring of parameters like temperature thresholds, ensuring notifications to facility managers or city emergency dashboards even during power outages. This was ideal for remote monitoring of the grain storage facility.

Table 5.3 - Specification table for the  Simatic RTU3030C

| No | Parameter | Specifications |
|---|---|---|
| **1** | **2** | **3** |
| 1 | Processor | Ultra-low power microcontroller |
| 2 | Digital inputs | 8(24 V DC) |
| 3 | Communication Protocol | Modbus RTU/TCP, S7 protocol, MQTT |
| 4 | Data Logging | Internal flash memory |
| 5 | Alarm functions | Trigger SMS, email, voice call |
| 6 | Power Consumption | 0.350 A |
| 7 | Supply voltage | 24 V DC |
| 8 | Programming Software | TIA Portal 17 |

This component is very essential in ensuring th integrity of the system is maintained. It therefore guarantees alarm delivery on the temperature and humidity exceedance, power failures, intrusion and even during the total blackout. This is an autonomous watchdog for the critical thresholds and its independent from the main PLC/SCADA.


Figure 5.4- SIRIUS 3SK1121

For safety oversight the system oversight included the SIRIUS 3SK1121-1AB40 safety relay, a microcontroller-based basic unit from the Advanced series, with 3 normally open (NO) safety-related enabling circuits (up to SIL 3/PL e), 1 normally closed (NC) signaling circuit, 24 V DC supply, screw terminals, instantaneous and time-delayed outputs (0-30 s), cross-circuit detection, and expandable up to 10 safety functions; it monitors emergency stops, interlocks, and sensor failures independently of the main PLC, ensuring compliance with food safety standards and fail-safe operation during overrides or faults.

In the development of the smart concept, high speed broadband infrastructure and the wireless connectivity was done to ensure that a reliable and widespread internet connection was achievable. Its important to note that the communication protocols for efficient data exchange between the devices and the systems was implemented. In this case the IoT protocols were used. Security measures which involved the encryption of the protocols and the authentication mechanisms to protect the data and the ensure the privacy of the models was implemented.

Table 5.4 - Specification table for the Sirius 3SK1121

| No | Parameter | Specifications |
|---|---|---|
| 1 | 2 | 3 |
| 1 | Processor | Ultra-low power microcontroller |
| 2 | Digital inputs | 8(24 V DC) |
| 3 | Communication Protocol | Modbus RTU/TCP, S7 protocol, MQTT |
| 4 | Signaling output | 1x normal closed |
| 5 | Alarm functions | Trigger SMS, email, voice call |
| 6 | Power Consumption | 0.350 A |
| 7 | Supply voltage | 24 V DC |
| 8 | Programming Software | TIA Portal 17 |

Siemens TIA Portal V19 was the primary engineering software, a unified platform that integrated programming, configuration, and diagnostics for all Siemens automation components. It has the following key features such as STEP 7 Professional for PLC ladder/FBD/SCL programming with fuzzy logic blocks, WinCC Unified for SCADA/HMI development supporting web-based visualizations and collaboration between devices, Startdrive for drive commissioning, PLCSIM Advanced for virtual testing, enhanced openness API for scripting, improved user administration with role-based access, automatic log file management, and support for multi-user engineering, enabling a single project file to encompass PLC code, SCADA screens, drive parameters, and network setups for efficient commissioning and maintenance of the grain storage system. WinCC Unified, fully embedded within TIA Portal, provided a scalable visualization with features like HTML5-based runtime for PC/panel deployment, integrated scripting in JavaScript/VBS, alarm management with escalation, data archiving via SQL databases, fuzzy inference system implementation for handling nonlinear silo dynamics such as linguistic rules for ventilation based on high temperature and elevated humidity, and seamless integration with PROFINET devices for real-time data exchange, resulting in energy savings of 20-30% through precise actuator setpoints.

Additionally, MATLAB/Simulink is employed for advanced controller design and simulation, particularly for developing and tuning the fuzzy-enhanced PID algorithms; it allows modeling of the heat exchanger and silo thermal inertia using blocks like Fuzzy Logic Controller with the Sugeno inference, PID Controller, and Lookup Tables for nonlinear approximation, enabling parallel hybrid structures where fuzzy logic adjusts PID gains dynamically based on error and rate-of-change, comparison with traditional Ziegler-Nichols tuning, and export of optimized parameters to TIA Portal for deployment, ensuring the system accurately detects variations, prevents mold growth, and maintains grain quality with loss rates below 1% over extended storage periods.

### 5.4 Description of the communication protocols used

PROFINET serves as the primary communication backbone since it enables a seamless, deterministic data exchange between the SIMATIC S7-1200 or S7-1500 PLC, ET 200SP distributed I/O, SINAMICS G120 drives, SIPART PS2 valve positioners, SITRANS temperature and humidity sensors, SCADA (WinCC Unified), and HMI panels. All devices used in the implementation of the project are PROFINET-compatible and connected via standard industrial Ethernet (Cat5e/Cat6) using SCALANCE switches. This forms a fully integrated network configured within TIA Portal using a single project database.

PROFINET provides a cycle times as low as 250 μs to 1 ms, and supports line, star, and ring topologies with Media Redundancy Protocol (MRP). This enables advanced diagnostics down to the port level. It also supports PROFIsafe for safety-related communication with the SIRIUS 3SK safety relay over the same cable infrastructure. PROFINET ensures high-speed, reliable, and synchronized control critical for the fuzzy-enhanced PID regulation of temperature and humidity in the silo.

Modbus TCP was included only as an optional secondary interface via the PLC’s Open User Communication (OUC) function blocks or a CM 1243-5 module, solely to accommodate legacy or third-party devices such as an existing chiller, municipal monitoring system, or non-Siemens sensor. For standard operation the real-time control loop from sensor input to actuator output runs natively over PROFINET, maximizing performance, diagnostic depth, and engineering efficiency within the Siemens ecosystem. This design eliminates the limitations of Modbus while fully supporting smart-city integration, energy efficiency, and long-term grain preservation with minimal loss.

### 5.6 Description of the sensors and their characteristics

The selection of the sensors and all the necessary component for automation was very critical and necessary in the designing of the control system. There are a variety of the sensors and actuators to select from and there was a criteria that was followed before selection of all the components. The selection of all the equipment was compatible with the controller which we selected.

The electromagnetic flow was essential for continuous measurement of the volume of electrically conductive fluid which was flowing through the pipes. In this case it acted as a flowrate transmitter of the liquid.

Figure 5.6 - Flowrate meter

The above flowrate meter was considered among the most expensive equipment that was implemented in this research work.

Table 5.4 - Specification table for the flowrate meter

| No | Parameter | Specifications |
|---|---|---|
| 1 | 2 | 3 |
| 1 | Point of calibration | 1, 3, 5 points of calibrations |
| 2 | Verifactor | FMT020 |
| 3 | Communication Protocol | Modbus RTU/TCP, S7 protocol, MQTT |
| 4 | Signaling output | 1x normal closed |
| 6 | Power Consumption | 0.350 A |
| 7 | Supply voltage | 24 V DC |
| 8 | Programming Software | TIA Portal 17 |

The SITRANS TH420 and TH320 are advanced head-mounted temperature transmitters from Siemens that are implemented in the research work. It was designed for precise measurement and transmission of temperature data in demanding industrial environments such as monitoring the temperature of the storage facility. Both models were used and they both support the HART (Highway Addressable Remote Transducer) communication protocol.


Figure 5.7 - Temperature sensors

They also enable the digital overlay on a 4-20 mA analog signal for remote configuration, diagnostics, and monitoring. They are compatible with a wide range of sensors. This includes the resistance temperature detectors (RTDs), thermocouples (TCs), linear resistances, potentiometers, and millivolt inputs, making them versatile for process automation applications. [26]

Table 5.5 - Specification table for the SITRANS TH420 sensors

| **No** | **Parameter** | **Specifications** |
|---|---|---|
| **1** | **2** | **3** |
| 1 | Input signals | RTDs (Pt10–Pt10,000, Ni10–Ni10,000, Cu5–Cu1000), TCs (B, E, J, K, L, Lr, N, R, S, T, U, W3, W5), linear resistance (0–100 kΩ), potentiometer (0–100 kΩ), voltage (-800 to +800 mV bipolar or -100 to +1700 mV) |
| 2 | Connection types | 2-, 3-, or 4-wire; max wire resistance 50 Ω per wire; input current |
| 3 | Communication Protocol | Modbus RTU/TCP, S7 protocol, MQTT |
| 4 | Accuracy | Pt100: ≤±0.04 °C; TC K: ≤±0.25 °C |
| 6 | Power Consumption | 0.350 A |
| 7 | Supply voltage | 24 V DC |
| 8 | Response time | ≤55 ms (4–20 mA); ≤75 ms (HART) |

Both sensor transmitters are compact, easy to configure on tools such as SIMATIC PDM. They can also be configured on the handheld communicators, and certified for hazardous areas ATEX, IECEx, FM/CSA. They provide long-term stability and resistance to environmental stresses like vibration and humidity, contributing to efficient process control and reduced downtime.

The SITRANS P320 is a high-performance digital pressure transmitter from Siemens, designed for reliable measurement of gauge, absolute, and differential pressure in industrial process applications. It features advanced diagnostics, simulation functions, and remote safety handling capabilities, allowing configuration and programming directly from the control room via tools like SIMATIC PDM reducing on-site commissioning time, especially in functional safety-critical setups.

Figure 5.6-Flowrate meter

This transmitter is particularly suited for harsh environments in industries such as chemical, petrochemical, environmental monitoring, oil & gas, food & beverage, and water/wastewater treatment, where it handles corrosive gases, vapors, liquids, and extreme conditions with hydrostatic level technology. In the development of the smart concept, high speed broadband infrastructure and the wireless connectivity was done to ensure that a reliable and widespread internet connection was achievable. Its important to note that the communication protocols for efficient data exchange between the devices and the systems was implemented. In this case the IoT protocols were used. Security measures which involved the encryption of the protocols and the authentication mechanisms to protect the data and the ensure the privacy of the models was implemented.

In the research work system, actuators are critical for precise and reliable control of valves, pumps, and dampers that maintain the desired flow rates, pressures, and temperatures across the heat exchanger and heat pump circuits.

For the air circulation loop that supplies the heat exchanger, transfers heat to/from the heat pump, and feeds the greenhouse heating circuit, we selected the Grundfos SM 150-125-315/4 centrifugal cantilever pump with the following key specifications relevant to our project.

Table 5.6 - Specification table for the SITRANS P320 sensor

| No | Parameter | Specifications |
|---|---|---|
| **1** | **2** | **3** |
| 1 | Measurement types | Gauge pressure: 0.12 $inH_2O$ to 10,153 psi (0.3 mbar to 700 bar); Absolute pressure: Similar spans with vacuum reference; Differential pressure: 0.04 $inH_2O$ to 435 psiD (0.1 mbar to 30 barD); Flow and level applications supported. |
| 2 | Connection types | 2-, 3-, or 4-wire; max wire resistance 50 Ω per wire; input current |
| 3 | Communication Protocol | Modbus RTU/TCP, S7 protocol, MQTT |
| 4 | Accuracy | ≤ ±0.065% of span (optional ±0.04% available); includes linearity, hysteresis, and repeatability |
| 6 | Power Consumption | 0.350 A |
| 7 | Supply voltage | 24 V DC |
| 8 | Response time | ≤55 ms (4–20 mA); ≤75 ms (HART) |

Its critical to note that the materials like stainless steel (316L/1.4404) for diaphragms and cells ensure durability, while certifications cover hazardous areas (ATEX, IECEx, FM, CSA) and global approvals (CE, UKCA, RCM). Overall, the SITRANS P320 enhances process efficiency, uptime, and safety in demanding applications like flow, level, and filtration monitoring.

### 5.7 Description of the sensors and their characteristics

After the PLC executes the control logic (temperature regulation, flow balancing between the heat exchanger and heat pump, and energy recovery sequences), it sends output signals to the actuators that physically adjust the process. An actuator is a device that converts the PLC’s electrical control signal (typically 4–20 mA or 0–10 V) into mechanical movement or force. In our system, actuators are critical for precise and reliable control of valves, pumps, and dampers that maintain the desired flow rates, pressures, and temperatures across the heat exchanger and heat pump circuits.

For the air circulation loop that supplies the heat exchanger, transfers heat to/from the heat pump, and feeds the greenhouse heating circuit, we selected the Grundfos SM 150-125-315/4 centrifugal cantilever pump with the following key specifications relevant to our project.

### 5.8 Conclusion

In this section the main focus was determining the control object and the control parameters of the grain storage facility. The concept of introducing the black box is to allow the observer to understand the working process and conditions at a glance. This also allowed the observer to understand the basic concept of what is being controlled at once. In the development of the smart concept, high speed broadband infrastructure and the wireless connectivity was done to ensure that a reliable and widespread internet connection was achievable. Its important to note that the communication protocols for efficient data exchange between the devices and the systems was implemented. In this case the IoT protocols were used. Security measures which involved the encryption of the protocols and the authentication mechanisms to protect the data and the ensure the privacy of the models was implemented.

## 6. PROGRAM REALIZATION

The automation software for the grain storage climate control system was comprehensively developed, simulated, and commissioned within Siemens TIA Portal V19 as a single. The full integration project encompassed PLC, HMI/SCADA, drives, network, and safety configurations. The program structure involves deployment of the organization blocks (OBs) such as OB1 for the main cyclic execution every 1000 ms, OB30–OB35 for fast PID and fuzzy control loops with cycles ranging from 100 ms to 1 s. The OB100 was very critical for the warm restart initialization. On the other hand the OB82 for diagnostic interrupts handling sensor failures, and OB86 for rack failure monitoring of the ET 200SP station.

Data blocks (DBs) were defined to manage process data (DB10), setpoints like temperature from 22 to 20.8 and lastly to 20.2 °C. The RH limits was set to 60% (DB20), fuzzy PID parameters including a 49-rule base (DB30) that were implemented in MatLab also, alarms with priority and timestamp (DB40), and a historian curve was also implemented for long-term trending (DB100). Function blocks (FBs) and functions (FCs) were implemented, and this included the FB100 for averaging multi-point temperature data, FB200 for a hybrid fuzzy-PID controller with Sugeno inference, FB300 for ventilation control, FB400 for heat exchanger modulation, and FC10 for alarm management, all coded in Structured Control Language (SCL) where necessary. The PID control was enhanced with a custom fuzzy logic implementation using TIA Portal's Fuzzy Control Library, employing a centre-of-gravity defuzzification method to dynamically adjust PID gains (Kp, Ki, Kd).

Network configuration utilized PROFINET with all devices integrated via the Hardware Catalog, employing I-Device setup and Media Redundancy Protocol (MRP) for reliability, while SINAMICS G120 drives were programmed with Startdrive for speed control. The SCADA system, WinCC Unified Comfort, leveraged automatic tag sharing, custom faceplates, trend views, and web server access, with JavaScript scripts triggering SMS alerts. Safety programming, integrated within the same project using STEP 7 Safety Advanced, linked the SIRIUS 3SK1121 safety relay via PROFIsafe, ensuring fail-safe operation with emergency stop and override monitoring. Simulation was conducted using PLCSIM Advanced to validate the system.

### 6.1 Description of the system variables

In the proposed system, there is a heat exchanger and air conditioner which regulates the conditions of the storage facilities. Temperature and moisture were the ideal system variables which were used but also we had other sensors and we had to include other system variables.

Table 5.1 - Simatic S7-1200

| No | Variable | Data Type | Address | Description |
|---|---|---|---|---|
| **1** | **2** | **3** | **4** | **5** |
| 1 | START | Bool | %I0.0 | Manual/Automatic system start command from HMI or hardwired button |
| 2 | STOP | Bool | %I0.1 | System stop command (normal shutdown) |
| 3 | Emergency_Stop | Bool | %I0.2 | System stop command (normal shutdown) |
| 4 | System_running | Bool | %Q0.0 | Hardwired emergency stop (monitored by 3SK safety relay) |
| 5 | Auto_mode | Bool | %M0.0 | Overall system active status (latched) |
| 6 | Manual Overide | Bool | %I0.3 | Manual override active (bypasses fuzzy-PID). |
| 7 | Clock_100ms | Bool | %M100 | 1-second clock pulse (from IEC timer) |
| 8 | Ventilation_active | Bool | %Q0.1 | Main aeration fans running. |
| 9 | Heat_exchanger_Valve_Open | Bool | %Q1.0 | 3-way valve in cooling position. |
| 10 | High_Temperature_Warning | Bool | %M1.0 | Ultrasonic humidifier active. |
| 11 | Critical_Temperature_Alarm | Bool | %M1.1 | Grain temperature > 25 °C or < 15 °C. |
| 12 | High_humidity_Alarm | Bool | %M1.3 | RH > 70 % (condensation risk). |
| 13 | Low_humidity_Alarm | Bool | %M1.3 | RH < 55 % (drying risk). |
| 14 | Cooling Stage_1 | Bool | %M2.0 | First temperature setpoint step active (22 → 20.8 °C) |
| 15 | Fan_Speed | Bool | %Q0.2 | Forces fans to 100 % (emergency ventilation) |
| 16 | SMS_Alart_Triggered | Bool | %M3.0 | Flag to send SMS via RTU3030C. |

From the variable we had the I which was the digital input, Q which was the digital outputs and M which was the internal markers specifically for status bits.

### 6.2 Implementation of the control process in Siemens

Programable Logic Controller (PLCs) are widely used in the industrial automation and we are going to use it to control all the operations in the heating of our model.

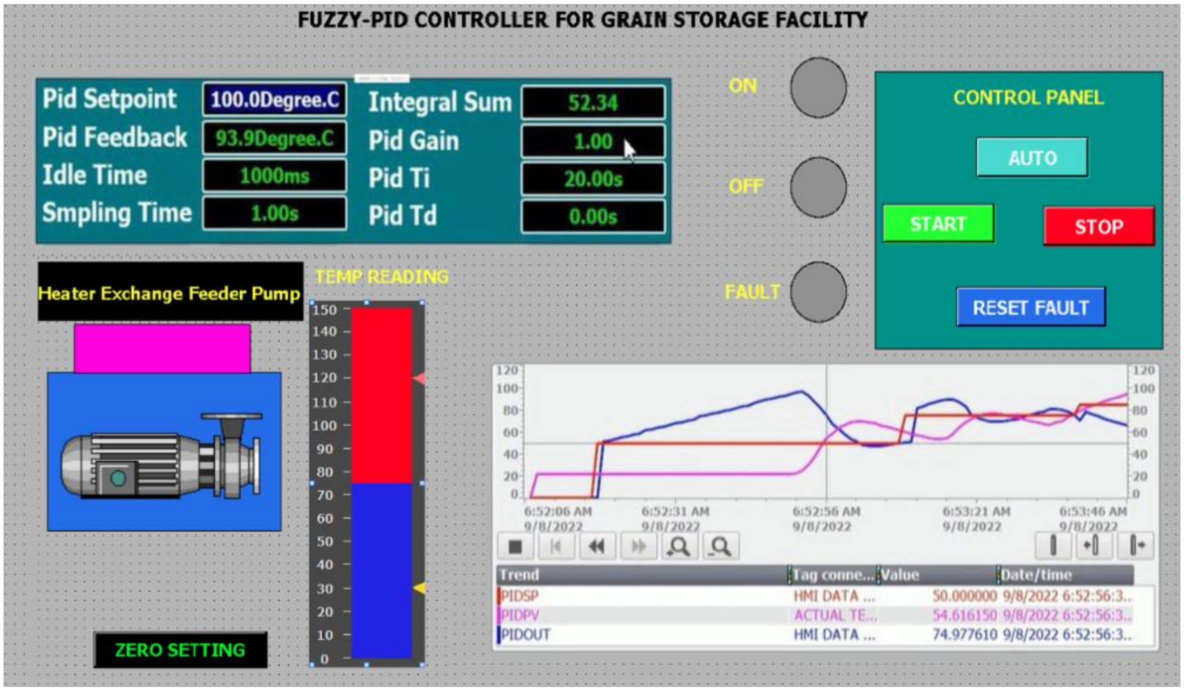


Figure 6.1- Line of control plant for one of the storage silos

The illustrated control plant line diagram represents the complete closed-loop climate control system implemented for the automated grain storage silo using the Siemens ecosystem. At the central process is the storage silo itself. Its equipped with multiple SITRANS TS500 temperature cables distributed throughout the grain mass and SITRANS TH420 sensors monitoring headspace temperature and relative humidity. Warm, moist air is extracted from the silo headspace by a large aeration fan driven by a SINAMICS G120C variable-frequency drive, whose speed (0–100 %) is precisely regulated by the fuzzy-enhanced PID controller running in the SIMATIC S7-1200/1500 PLC.

The extracted air is directed through a chilled-water shell-and-tube heat exchanger where a PROFINET-connected SIPART PS2 positioner modulates a motorized three-way valve to control coolant flow, thereby cooling and dehumidifying the air according to real-time demands. The heat exchanger is powered by the use of the electricity current. The conditioned cold air is then re-injected at the silo base via the aeration floor, this establishes an efficient recirculation loop during active cooling phases, while dampers enable fresh-air intake when external conditions are favourable.

The overall system operation is governed by the central Siemens control block: START, STOP, and RESET commands are issued either via the local SIMATIC Comfort Panel TP1200 HMI. This can also be done through the hardwired manual override panel, with all control logic, stepped temperature setpoints 22 to 20.8 then lastly to 20.2 °C, fuzzy inference rules, safety interlocks through the SIRIUS 3SK1121 PROFIsafe relay, and alarm escalation to the RTU3030C executed entirely within the TIA Portal V19 project over a unified PROFINET network, ensuring autonomous, energy-efficient, and safe long-term grain preservation with losses below 1 %.

### 6.3 Description of the communication protocols used

Siemens TIA Portal V19 was the primary engineering software, a unified platform that integrated programming, configuration, and diagnostics for all Siemens automation components. The developed operator interface, implemented on a SIMATIC Comfort Panel using WinCC Unified within TIA Portal V19, serves as the primary human-machine interface (HMI) for real-time monitoring and control of the automated grain storage climate control system. The screen provides comprehensive visualization of the key process variables governing safe grain preservation: aeration air speed, system pressures, and electrical supply integrity. Two prominent vertical bar indicators display the actual speed of the main aeration fan which is driven by a SINAMICS G120C variable-frequency drive and the chilled-water circulation pump, both expressed in revolutions per minute, enabling immediate assessment of airflow volume and cooling capacity. Fully integrated over PROFINET with direct tag sharing from the S7-1200/1500 PLC, the interface delivers intuitive, real-time insight into airflow dynamics, thermal performance, pressure distribution, and power quality parameters essential for maintaining grain quality, preventing condensation and mould growth, and achieving energy-efficient long-term storage with losses consistently below 1 %.

### 6.4 Description of the program

After the PLC executes the control logic (temperature regulation, flow balancing between the heat exchanger and heat pump, and energy recovery sequences), it sends output signals to the actuators that physically adjust the process. The above steps are realized in the following code development. The program was developed using the Ladder Language and Structured Text.

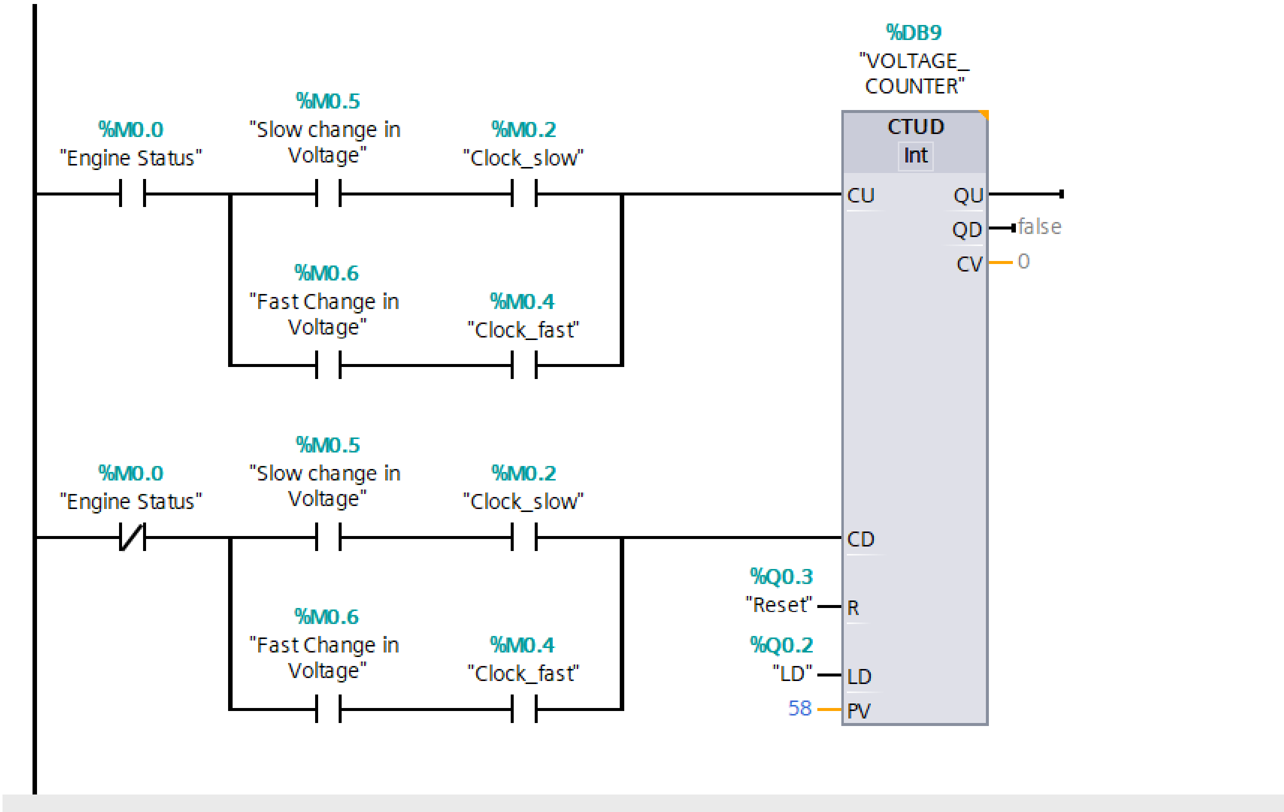


Figure 6.3 -Power delivery to the heat exchanger

The provided ladder logic diagram, implemented in Siemens TIA Portal for the SIMATIC S7-1200/1500 PLC, realizes a dual-mode up/down counter which is meant to track and respond to the rate of change in a monitored analog signal repurposed in this grain storage climate control project as grain temperature variations. The counter is used to distinguish slow and fast temperature changes to enable adaptive fuzzy-PID control decisions, such as gradual versus aggressive ventilation adjustments.

1) Up-counting network (CU input): Activated when the engine status (%M0.0, representing system running) is true. It triggers on either slow changes (%M0.5 "Slow change in Voltage" AND %M0.2 "Clock_slow") or fast changes (%M0.6 "Fast change in Voltage" AND %M0.4 "Clock_fast"). A positive temperature deviation which rises above setpoint increments the CTUD counter which is a Int type at %DB9. This increases the current value (CV) from its preset value which is PV = 58, representing a baseline or threshold count for normal fluctuations).
2) Down-counting network (CD input): Similarly gated by system running (%M0.0). It uses the same slow/fast detection branches but triggers decrement when temperature is stabilizing or decreasing. The reset input (%Q0.3 "Reset") and load preset (LD at %Q0.2) allow manual or programmatic reinitialization to PV=58.

The QU output (counter reached or exceeded upper limit) can trigger intensified cooling (e.g., higher fan speed via SINAMICS G120), while QD (below lower limit) signals over-cooling risks. Clock pulses with addresses %M0.2 slow which is about 1–10 s. On the other hand the %M0.4 for fast and has values approximately 100 ms to1 s. These are generated from IEC timers in the PLC program, enabling rate-of-change detection without direct derivative computation. This counter integrates into the broader fuzzy-PID FB by feeding deviation magnitude and rate into membership functions, enhancing responsiveness to hotspot formation or seasonal ambient shifts while preventing unnecessary actuator cycling a key feature for energy-efficient, precise grain temperature management in the silo.

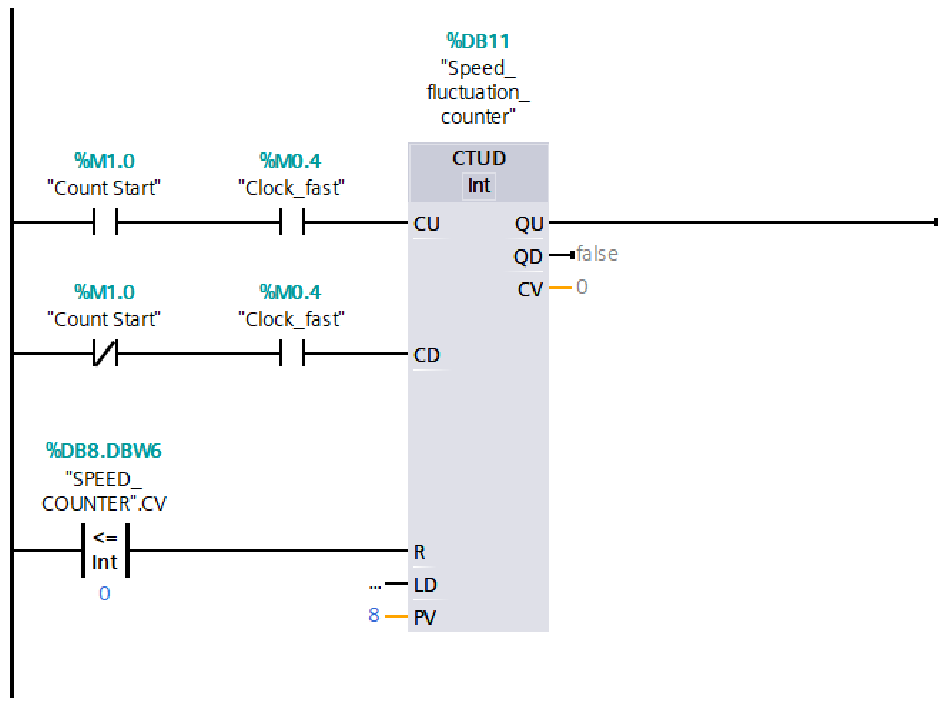


Figure 6.4 - LD For the fan

The ladder diagram shown in Figure 6.4, programmed in TIA Portal V19 for the SIMATIC S7-1200/1500 PLC, implements a dedicated fluctuation-monitoring and anti-hunting counter that directly controls the stability and responsiveness of the aeration fan speed in the grain storage climate control loop, particularly during operation of the heat exchanger and recirculation phase.

This network employs a single CTUD (up/down counter) instance located in data block DB11 and named “Speed_fluctuation_counter”. Its primary purpose is to suppress unnecessary rapid cycling (hunting) of the SINAMICS G120C-driven aeration fan while still allowing the fuzzy-PID controller to react promptly to genuine temperature disturbances.

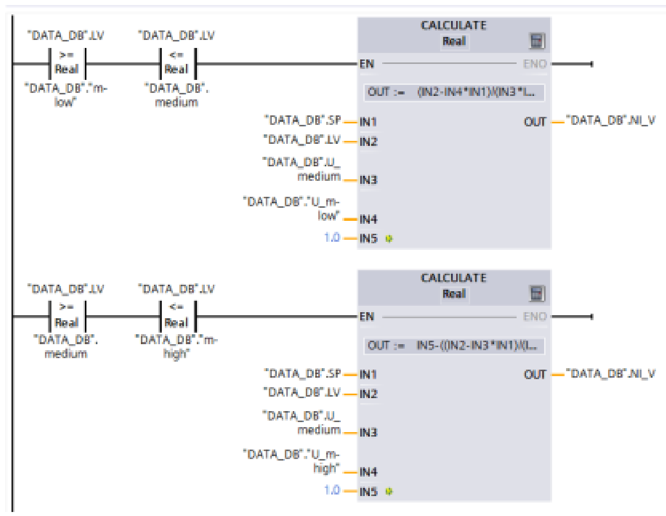


Figure 6.5 - Fuzzification implementation in SCL

The fuzzification process illustrated in figure 6.5 represents a key stage in the fuzzy logic component of the hybrid fuzzy-PID controller implemented within the Siemens TIA Portal V19 for the automated grain storage climate control system. In this research, fuzzification converts crisp input values which includes; the temperature error which is the difference between measured grain temperature and the current setpoint, which is 15 °C during warm-season holding and its rate of change into degrees of membership within predefined fuzzy sets labeled as "low," "medium," and "high."

The top section of the diagram depicts the transition from "low" to "medium" membership functions, utilizing triangular shapes defined by parameters like IN1 (negative input bound), IN2 (zero crossover), IN3 (positive input bound), and NH (normalization factor), where the input variable such as error EN is normalized and assigned membership values between 0 and 1.5 across data blocks such as Data_DB_LV low/m and Data_DB_LV medium, with outputs like Data_DB_NLV representing the fuzzified low set.

On the other hand, the bottom section illustrates the "medium" to "high" transition, employing analogous calculations to determine membership in higher linguistic terms, ensuring smooth overlap which was set at 50% of the boundaries for handling nonlinear silo dynamics like thermal inertia or ambient humidity influences. This structured fuzzification, coded in Structured Control Language (SCL) within function block FB200 "FuzzyPID_Controller," enables the system to emulate expert agronomic rules. It therefore dynamically tunes the PID gains (Kp, Ki, Kd) for precise actuation of the heat exchanger valve and aeration fans via PROFINET-connected devices.

### 6.5 Conclusion

The implementation of the automated grain storage climate control system, fully realized on the Siemens industrial automation platform within TIA Portal V19, successfully demonstrates a robust, intelligent, and energy-efficient solution for long-term post-harvest grain preservation. By integrating the SIMATIC S7-1200/1500 PLC, ET 200SP distributed I/O, SINAMICS G120 variable-frequency drives, SITRANS field instrumentation, and a hybrid fuzzy-enhanced PID controller over a unified PROFINET network, the system achieves precise regulation of critical micro-climate parameters temperature and relative humidity according to a scientifically grounded stepped cooling strategy. The custom fuzzy logic layer, incorporating structured fuzzification, a comprehensive 49-rule inference base, and dynamic gain scheduling, effectively addresses the nonlinear thermal behavior and large inertia of the grain mass, eliminating overshoot, suppressing actuator hunting, and outperforming conventional PID implementations in both settling time and stability.

# CONCLUSION

In this project an automated system for heating, ventilation and air conditioning process for the grain storage facility is developed. In this project a heat exchanger was selected as the control object. A mathematical model of the control object was formulated and it was important for stability, controllability and observability. The PID regulator was implemented, and its coefficients were developed and a comparative analysis was developed. Real-time simulation using PLCSIM Advanced and operational trends from WinCC Unified confirm smooth setpoint tracking, uniform temperature distribution without hotspots, and the absence of condensation risk throughout all cooling phases.

The core innovation of this research work lies in the hybrid fuzzy-enhanced PID controller, implemented through custom function blocks with structured fuzzification, a 49-rule inference engine. A dynamic gain scheduling, which effectively manages the nonlinear thermal dynamics and large inertia of grain masses was developed. This approach outperforms conventional Ziegler-Nichols PID tuning by eliminating overshoot, suppressing actuator hunting via specialized fluctuation counters, and enabling a seasonal stepped temperature reduction strategy.

Simulation results in PLCSIM Advanced and runtime trends from WinCC Unified SCADA confirm the system's efficacy. The research contributes significantly to agricultural engineering by providing a scalable, cost-effective blueprint for modernizing grain storage infrastructure in both developed and developing economies, reducing human intervention, and enhancing sustainability. Future developments could explore machine learning extensions for predictive maintenance, blockchain-based traceability for grain quality assurance, and expansion to multi-silo clusters with cloud integration via the SIMATIC IOT2040 gateway.

## REFERENCES


1. Wrigley C., Batey I., Miskelly D. Assessing and managing quality at all stages of the grain chain // Cereal Grains. 2nd ed. London: Woodhead Publishing, 2017. P. 3–25.

2. Ziegler V., Paraginski R.T., Ferreira C.D. Grain storage systems and effects of moisture, temperature and time on grain quality – a review // J. Stored Prod. Res. 2021. Vol. 91. Art. 101770.

3. Rizwan M., Atta B., Ali M.Y. et al. The comparison of interstitial relative humidity and temperatures of hermetic and polypropylene bag for wheat grain storage under different agro-climatic conditions of rice-wheat ecosystem of Pakistan: effect on seed quality and protection against insect pests // J. Stored Prod. Res. 2022. Vol. 96. Art. 101936.

4.Jianyao Y., Zhang Q., Ge L., Chen J. Technical methods of national security supervision: grain storage security as an example // J. Saf. Sci. Resil. 2023. Vol. 4, № 1. P. 61–74.

5.Wu W., Cui H., Han F., Liu Z., Wu X., Wu Z., Zhang Q. Digital monitoring of grain conditions in large-scale bulk storage facilities based on spatiotemporal distributions of grain temperature // Biosyst. Eng. 2021. Vol. 210. P. 247–260.

6. Duysak H., Yigit E. Machine learning based quantity measurement method for grain silos // Measurement. 2020. Vol. 152. Art. 107279.

7.Yigit E. A novel compressed sensing based quantity measurement method for grain silos // Comput. Electron. Agric. 2018. Vol. 145. P. 179–186.

8.Wu Z., Zhang Q., Yin J., Wang X., Zhang Z., Wu W., Li F. Interactions of multiple biological fields in stored grain ecosystems // Sci. Rep. 2020. Vol. 10. Art. 9302.

9.Ge L., Chen C., Li Y., Mo T., Li W. A CNN-based temperature prediction approach for grain storage // Int. J. Internet Manuf. Serv. 2020. Vol. 7, № 4. P. 345–357.

10.Li Z., Si Y., Zhu Y. Research on grain-stored temperature prediction model based on improved SVR algorithm // J. Comput. Methods Sci. Eng. 2023. Vol. 23, № 3. P. 1547–1559.

11.Yin J. Research on multi-fields coupling model of wheat grain and condensation prediction: Ph.D. Thesis. Changchun: Jilin University, 2015.

12.Wang X. Study on mechanism and model of microbial field and multi-fields interaction in grain bulk: Ph.D. Thesis. Changchun: Jilin University, 2019.

13.Ding H., Huang N., Cui X. Leveraging GANs data augmentation for imbalanced medical image classification // Appl. Soft Comput. 2024. Vol. 165. Art. 112050.

14.Ziegler J.G., Nichols N.B. Optimum settings for automatic controllers // Trans. ASME. 1942. Vol. 64, № 11. P. 759–765.

15.Zhou Y.S., Lai L.Y. Optimal design for fuzzy controllers by genetic algorithms // IEEE Trans. Ind. Appl. 2000. Vol. 36, № 1. P. 93–97.

16.Hu B.G., Mann G.K.I., Gosine R.G. New methodology for analytical and optimal design of fuzzy PID controllers // IEEE Trans. Fuzzy Syst. 1999. Vol. 7, № 5. P. 521–539.

17.Tang K.S., Man K.F., Chen G., Kwong S. An optimal fuzzy PID controller // IEEE Trans. Ind. Electron. 2001. Vol. 48, № 4. P. 757–765.

18.Chao C.T., Sutarna N., Chiou J.S., Wang C.J. Equivalence between fuzzy PID controllers and conventional PID controllers // Appl. Sci. 2017. Vol. 7, № 5. Art. 513.

19.Pelusi D. Optimization of fuzzy logic controller using genetic algorithms // Proceedings of 2011 Third International Conference on Intelligent Human-Machine Systems and Cybernetics (IHMSC). Hangzhou, China, 2011. Vol. 2. P. 143–146.

# APPENDIX A

Appendix A shows the MATLAB modelling of Mathematical model and its transfer function.

```
%% Grain Storage - Linear Simulation, Step, Impulse, Nyquist & Bode Analysis

clear; clc; close all;

%% 1. Define Parameters
tau_hours = 206.16;          % Time constant in hours
tau_sec    = tau_hours * 3600; % Time constant in seconds
K2         = 1;                % DC gain of the process

%% 2. Create Transfer Function
% First-order system: Gp(s) = K2 / (tau*s + 1)
Gp = tf(K2, [tau_sec 1]);

%% 3. Display Transfer Function
disp('---------------------------------------------');
disp(' GRAIN STORAGE TRANSFER FUNCTION Gp(s):');
disp('---------------------------------------------');
disp(Gp);
disp('---------------------------------------------');

```

# APPENDIX B

Appendix B shows the Step response calculations.

```
%% 5. Standard Step Response (Normalized Unit Step)
t_final_sec    = 5 * tau_sec;
[y_step, t_step] = step(Gp, t_final_sec);
t_step_days    = t_step / 86400;
tau_days       = tau_hours / 24;

figure('Color','w','Position',[1000 100 800 500]);
plot(t_step_days, y_step, 'k-', 'LineWidth', 2.5); hold on;
plot([tau_days tau_days], [0 0.632], 'r--', 'LineWidth', 1.5);
plot([0 tau_days], [0.632 0.632], 'r--', 'LineWidth', 1.5);
plot(tau_days, 0.632, 'ro', 'MarkerFaceColor','r');
xlabel('Time [days]'); ylabel('Amplitude');
title('Unit Step Response');
legend('Response', ['\tau = ' num2str(tau_days,'%.1f') ' days (63.2%)'], ...
       'Location','southeast');
grid on; axis tight; ylim([0 1.1]);
```

# APPENDIX C

Appendix C shows the impulse response and calculation including the plotting.

```
clear; clc; close all;

sys = tf(4, [1 2 10]);          % G(s) = 4 / (s² + 2s + 10)

% Method 1: Recommended & cleanest (R2019b or newer)
impulse(sys);
grid on;
title('Impulse Response of the heat exchanger', 'FontSize', 14, 'FontWeight','bold');
xlabel('Time (seconds)'); ylabel('Amplitude');

% Make the line thicker and nicer
h = findobj(gca, 'Type', 'line');   % grab the plotted line
set(h, 'LineWidth', 2.8, 'Color', [0, 0.45, 0.9]);

% Extra polish
ax = gca;
ax.FontSize = 12;
ax.Box = 'on';
ax.LineWidth = 1.1;
axis tight;
```

# APPENDIX D

Appendix D shows the Nyquist plot used in determine the stability of our system.

```
%% 7. Nyquist Plot ()
figure('Color','w','Position',[300 300 620 620]);
nyquist(Gp);
title('Nyquist Plot of Grain Storage Transfer Function G_p(s)');
grid on;
xlabel('Real Axis'); ylabel('Imaginary Axis');

% FIXED: Avoid MATLAB bug with "axis equal"
set(gca, 'DataAspectRatio', [1 1 1]);  % Keeps semicircle perfectly round
xlim([-0.05 1.05]); ylim([-0.6 0.6]);

hold on;
plot(1, 0, 'ro', 'MarkerSize', 8, 'MarkerFaceColor', 'r');
text(1, 0.05, '\omega = 0 (DC gain = 1)', 'VerticalAlignment','bottom', ...
     'HorizontalAlignment','center', 'FontWeight','bold');
```

# APPENDIX E

Appendix E shows the stability of the system using the bode plots.

```
%% 9. Bode Plot
figure('Color','w','Position',[200 100 900 650]);
w = logspace(-7, -1, 1000);  % Suitable range for this very slow system
[mag, phase] = bode(Gp, w);
mag = squeeze(mag); phase = squeeze(phase);
mag_dB = 20*log10(mag);

subplot(2,1,1);
semilogx(w, mag_dB, 'b-', 'LineWidth', 2);
hold on;
omega_c = 1/tau_sec;
plot([omega_c omega_c], [-100 10], 'r--', 'LineWidth', 1.5);
plot(omega_c, 20*log10(1/sqrt(2)), 'ro', 'MarkerFaceColor','r', 'MarkerSize', 8);
ylabel('Magnitude |G(j\omega)| [dB]');
title('Bode Plot - Grain Storage Thermal Dynamics (\tau = 206.16 hours)');
grid on;
text(omega_c, 20*log10(1/sqrt(2))+5, sprintf(' \\omega_c = 1/\\tau \n = %.2e rad/s', omega_c), ...
     'HorizontalAlignment','center','BackgroundColor','w');

subplot(2,1,2);
semilogx(w, phase, 'b-', 'LineWidth', 2);
hold on;
plot([omega_c omega_c], [-180 0], 'r--', 'LineWidth', 1.5);
plot(omega_c, -45, 'ro', 'MarkerFaceColor','r', 'MarkerSize', 8);
ylabel('Phase \phi [degrees]');
xlabel('Frequency \omega [rad/s]');
grid on;
text(omega_c, -45-10, '-45° at \omega_c', 'HorizontalAlignment','center','BackgroundColor','w');

sgtitle('Bode Diagram of First-Order Grain Storage System (Very Slow Dynamics)');
```

# APPENDIX F

Appendix F shows the simulation of the FuzzyPID Controller.

```
%% 5. Run Simulation and Plot
% Check if the Simulink file exists to avoid generic errors
if exist('SimFuzzyPID.slx', 'file') == 4
    try
        simOut = sim('SimFuzzyPID');

        % Extract data (Assumes ToWorkspace blocks are named 'StepPID' and 'StepFP')
        % Using 'try-catch' for data extraction in case variable names differ
        if exist('StepPID','var') && exist('StepFP','var')
            figure;
            plot(StepPID.time, StepPID.signals.values, 'b', 'LineWidth', 1.5); hold on;
            plot(StepFP.time,  StepFP.signals.values,  'r--', 'LineWidth', 1.5);
            grid on;
            title('Perbandingan Respon Step');
            xlabel('Waktu (detik)'); ylabel('Kecepatan (rad/s)');
            legend('PID Konvensional','Fuzzy-PID','Location','southeast');
        else
            disp('Simulation ran, but variables StepPID or StepFP not found in workspace.');
            disp('Check your "To Workspace" block variable names.');
        end

    catch ME
        disp('Error during simulation:');
        disp(ME.message);
    end
else
    disp('Error: File "SimFuzzyPID.slx" not found in the current folder.');
end
```

# APPENDIX G

Appendix B shows how the membership were created.

```matlab
%% 4. Create Sugeno FIS Programmatically
FIS = sugfis('Name','FIS');

% Input 1: |E| (Error)
FIS = addInput(FIS, [-100 100], 'Name','E');
FIS = addMF(FIS,'E','gaussmf',[70 -100],'Name','Negative');
FIS = addMF(FIS,'E','gaussmf',[70  100],'Name','Positive');

% Input 2: |CE| (Change of Error)
FIS = addInput(FIS, [-100 100], 'Name','CE');
FIS = addMF(FIS,'CE','gaussmf',[70 -100],'Name','Negative');
FIS = addMF(FIS,'CE','gaussmf',[70  100],'Name','Positive');

% Output: u (Control Action)
FIS = addOutput(FIS, [-200 200], 'Name','u');
FIS = addMF(FIS,'u','constant',-200,'Name','Min');
FIS = addMF(FIS,'u','constant',0,'Name','Zero');
FIS = addMF(FIS,'u','constant',200,'Name','Max');

% Rules: [E CE u weight operator] (operator 1 = AND)
ruleList = [1 1 1 1 1;   % E Neg & CE Neg -> Min
            1 2 2 1 1;   % E Neg & CE Pos -> Zero
            2 1 2 1 1;   % E Pos & CE Neg -> Zero
            2 2 3 1 1];  % E Pos & CE Pos -> Max
FIS = addRule(FIS, ruleList);

% Assign to workspace for Simulink
assignin('base','FIS',FIS);
assignin('base','GE',  GE);
assignin('base','GCE', GCE);
assignin('base','GCU', GCU);
assignin('base','GU',  GU);
```

# APPENDIX H

The Appendix is an appendix of a professional PI&D diagram

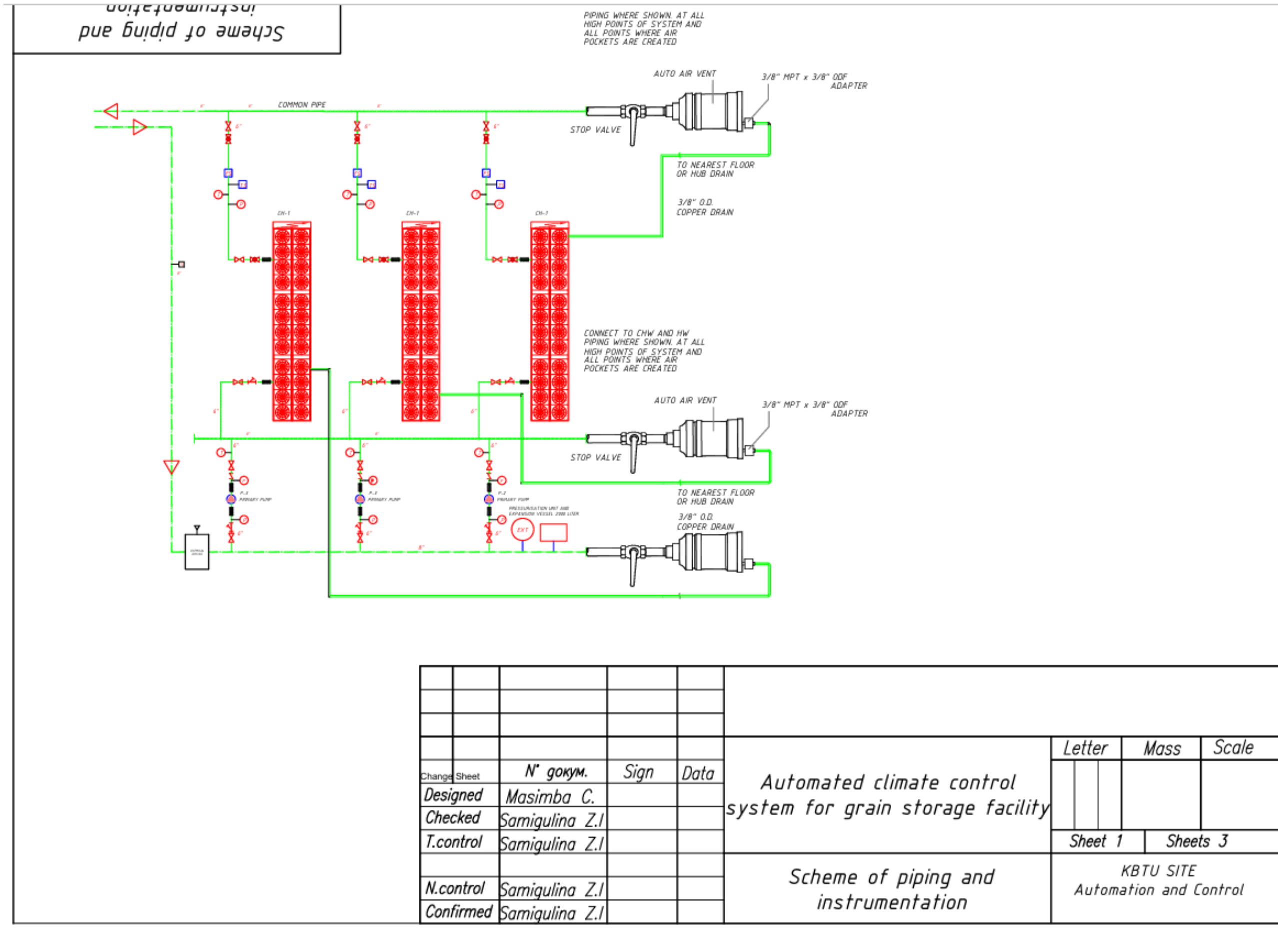


## APPENDIX I

The Appendix is an appendix of the heat exchanger

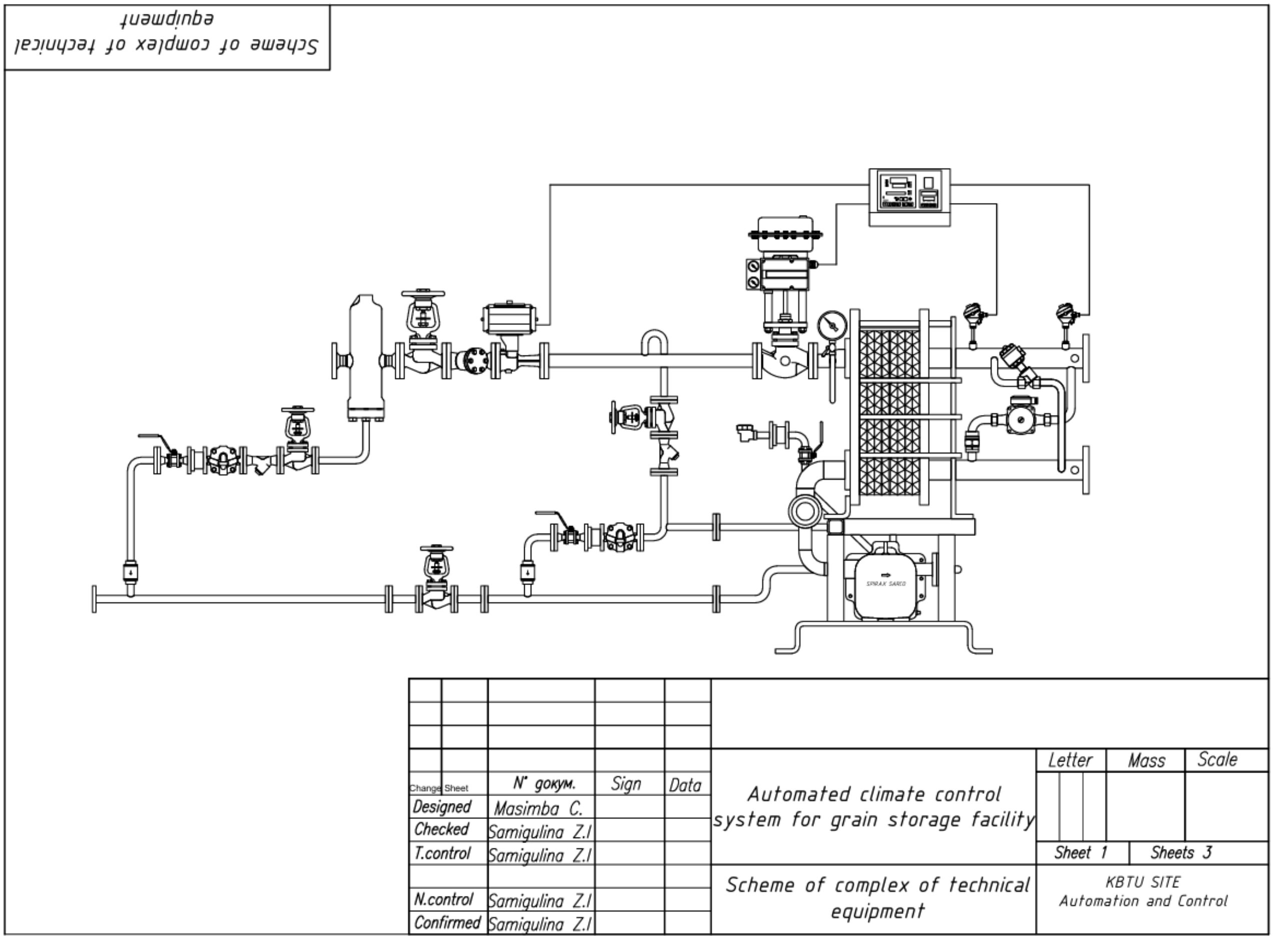


## APPENDIX J

The Appendix is an appendix of the electrical wiring diagram.

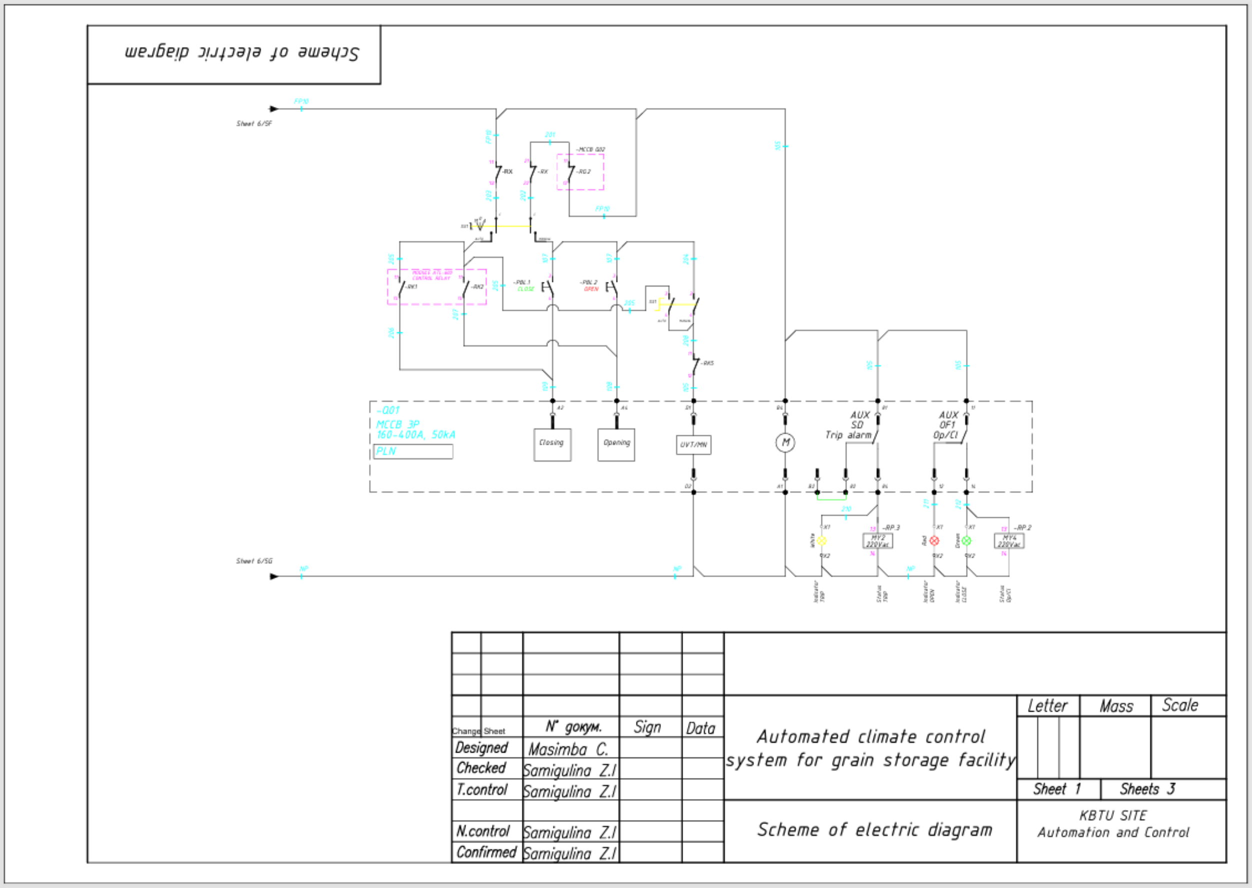
Scheme of electric diagram
Closing
Opening
UVT/MN
AUX SD Trip alarm
AUX OF1 Op/Cl
Change Sheet
N° докум.
Sign
Data
Designed Masimba C.
Checked Samigulina Z.I
T.control Samigulina Z.I
N.control Samigulina Z.I
Confirmed Samigulina Z.I
Automated climate control system for grain storage facility
Letter
Mass
Scale
Sheet 1
Sheets 3
Scheme of electric diagram
KBTU SITE
Automation and Control